THE JOURNAL OF BIOLOGICAL CHEMISTRY Vol. 279, No. 49, Issue of December 3, pp. 51107–51121, 2004
Printed in U.S.A.

A Dynamic Pool of Calcium in Catecholamine Storage Vesicles

EXPLORATION IN LIVING CELLS BY A NOVEL VESICLE-TARGETED CHROMOGRANIN A-AEQUORIN CHIMERIC PHOTOPROTEIN*

Received for publication, August 2, 2004, and in revised form, September 3, 2004
Published, JBC Papers in Press, September 9, 2004, DOI 10.1074/jbc.M408742200

Nitish R. Mahapatra‡, Manjula Mahata‡, Partha P. Hazra§¶, Patrick M. McDonough‡‖, Daniel T. O'Connor‡‡‡§§, and Sushil K. Mahata‡ ‡‡¶¶**

*From the ‡Department of Medicine, the §Division of Biology, and **Molecular Genetics, University of California, and the ‡‡Veterans Affairs San Diego Healthcare System, San Diego, California 92093-0838*

Chromaffin vesicles contain very high concentration of Ca^{2+} (~20–40 mM total), compared with ~100 nM in the cytosol. Aequorin, a jellyfish photoprotein with Ca^{2+}-dependent luminescence, measures $[Ca^{2+}]$ in specific subcellular compartments wherein proteins with organelle-specific trafficking domains are fused in-frame to aequorin. Because of the presence of vesicular trafficking domain within CgA we engineered sorting of an expressed human CgA-Aequorin fusion protein (hCgA-Aeq) into the vesicle compartment as confirmed by sucrose density gradients and confocal immunofluorescent co-localization studies. hCgA-Aeq and cytoplasmic aequorin (Cyto-Aeq) luminescence displayed linear functions of $[Ca^{2+}]$ *in vitro*, over >5 $\log_{10}$ orders of magnitude ($r > 0.99$), and down to at least 10^{-7} M sensitivity. Calibrating the pH dependence of hCgA-Aeq luminescence allowed estimation of $[Ca^{2+}]_{ves}$ at granule interior pH (~5.5). In the cytoplasm, Cyto-Aeq accurately determined $[Ca^{2+}]_{cyto}$ under both basal ($[Ca^{2+}]_{cyto}$ = 130 ± 35 nM) and exocytosis-stimulated conditions, confirmed by an independent reference technique (Indo-1 fluorescence). The hCgA-Aeq chimera determined vesicular free $[Ca^{2+}]_{ves}$ = 1.4 ± 0.3 μM under basal conditions indicating that >99% of granule total Ca^{2+} is in a "bound" state. The basal free $[Ca^{2+}]_{ves}/[Ca^{2+}]_{cyto}$ ratio was thus ~10.8-fold, indicating active, dynamic Ca^{2+} uptake from cytosol into the granules. Stimulation of exocytotic secretion revealed prompt, dynamic increases in both $[Ca^{2+}]_{ves}$ and $[Ca^{2+}]_{cyto}$, and an exponential relation between the two ($y = 0.99 \times e^{(1.53x)}$, $r = 0.99$), reflecting a persistent $[Ca^{2+}]_{ves}/[Ca^{2+}]_{cyto}$ gradient, even during sharp increments of both values. Studies with inhibitors of Ca^{2+} translocation (Ca^{2+}-ATPase), Na^+/Ca^+-exchange, Na^+/H^+-exchange, and vesicle acidification (H^+-translocating ATPase), documented a role for these four ion transporter classes in accumulation of Ca^{2+} inside the vesicles.

Catecholamine storage vesicles (chromaffin granules) contain quite substantial concentrations of catecholamines (~0.6 M), adenosine triphosphate (ATP, ~150 mM), Ca^{2+} (~20–40 mM), and chromogranins (~2–4 mM) in their soluble cores (1–3). The granule accumulation of Ca^{2+}, at ~20–40 mM total concentration, is in striking contrast to the ~100 nM Ca^{2+} concentration in the cytosol, suggesting that a Ca^{2+} concentration gradient of up to ~10^5-fold might occur across the granule membrane. However, little is known about the processes that might underlie Ca^{2+} accumulation in secretory granules, the fraction of granule Ca^{2+}, which is free (*versus* bound) is not well understood, and no tools currently exist to measure $[Ca^{2+}]$ *in situ* within chromaffin granules in living cells.

An increment in cytosolic $[Ca^{2+}]$ is a prerequisite for exocytotic secretion of catecholamines (4, 5). Besides stimulation of exocytosis, Ca^{2+} also plays a central role in regulating a variety of neuronal processes, such as cytoskeletal dynamics, gene expression (6–8), and signal transduction (5, 9). Influx of Ca^{2+} from either the extracellular space (4, 10) or intracellular stores, such as endoplasmic reticulum (11) or mitochondria (12, 13), may influence cytosolic $[Ca^{2+}]$.

Changes in cytoplasmic $[Ca^{2+}]$ can be monitored by introducing Ca^{2+}-chelating fluorescent dyes such as Indo-1 (5, 14) or Fura-2 (15, 16) into the cytosol. These fluorescent dyes can quantify $[Ca^{2+}]$ in the cytosol, but their intracellular diffusion precludes their use to measure $[Ca^{2+}]$ in particular organelles. The jellyfish (*Aequoria victoria*) green fluorescent protein (GFP)[1] has been engineered to detect cytoplasmic $[Ca^{2+}]$ by fluorescent resonant energy transfer (FRET) of chimeric donor/acceptor GFP modules in response to Ca^{2+} binding (17), but severe fluorescence intensity quenching of one or the other of the donor/acceptor GFP modules at the very acidic chromaffin granule interior pH of ~5.5 (18, 19) precludes use of this method in the granule (17).

The jellyfish photoprotein apoaequorin (~21–22 kDa) forms a complex with its cofactor coelenterazine and molecular oxygen; binding of calcium at three specific aequorin sites permits oxidation of colenterazine to coelenteramide, yielding a photon at ~466 nm by luminescence (20). This aequorin luminescence

* This work was supported by grants from the Department of Veterans Affairs and the National Institutes of Health. The costs of publication of this article were defrayed in part by the payment of page charges. This article must therefore be hereby marked "*advertisement*" in accordance with 18 U.S.C. Section 1734 solely to indicate this fact.

¶ Present address: Biocon Limited, 20th K. M. Hosur Rd., Electronic City P. O. Bangalore-560100, India.

‖ Present address: Dept. of Biology, San Diego State University, 5500 Campanile Dr., San Diego, CA 92182.

§§ To whom correspondence may be addressed: Dept. of Medicine, University of California at San Diego, and VASDHS (0838), 9500 Gilman Dr., La Jolla, CA 92093-0838. Tel.: 858-5528585 (ext. 7373); Fax: 858-642-6425; E-mail: doconnor@ucsd.edu.

¶¶ To whom correspondence may be addressed: Dept. of Medicine, University of California at San Diego, and VASDHS (0838), 9500 Gilman Dr., La Jolla, CA 92093-0838. Tel.: 858-5528585 (ext. 2637); Fax: 858-642-6425; E-mail: smahata@ucsd.edu.

[1] The abbreviations used are: GFP, green fluorescent protein; Aeq, aequorin (jellyfish photoprotein with Ca^{2+}-dependent luminescence); $[Ca^{2+}]$, Ca^{2+} concentration; $[Ca^{2+}]_{cyto}$, cytoplasmic free $[Ca^{2+}]$; $[Ca^{2+}]_{ves}$, chromaffin vesicle interior free $[Ca^{2+}]$; CgA, chromogranin A; Cyto-Aeq, cytoplasmic aequorin (with no additional targeting signals); DBH, dopamine β-hydroxyase; hCgA, human chromogranin A; hCgA-Aeq, chimera of human chromogranin A fused in-frame to aequorin; NCX, Na^+/Ca^{2+} exchanger (antiporter, counter-transporter); NHE, Na^+/H^+ exchanger (antiporter, counter-transporter); PBS, phosphate-buffered saline; NGF, nerve growth factor; MES, 2-morpholinoethanesulfonic acid; MOPS, 4-morpholinepropanesulfonic acid.

can be quantified by a photomultiplier tube in the dark and its strict calcium dependence has been used to measure local calcium concentration in particular subcellular depots to which aequorin has been steered by exploiting the intracellular trafficking information in appropriately selected fusion proteins (21); successful examples include targeting to endoplasmic reticulum (22), mitochondria (23), Golgi apparatus (24), or nucleus (25). Such targeted recombinant aequorins provide the most specific means of monitoring free [Ca^{2+}] in particular subcellular compartments.

Chromogranin A (CgA) is the major protein in the soluble core of chromaffin granules (1, 3) and its N terminus has been suggested to contain the targeting signal for trafficking to chromaffin granules (26, 27). Therefore, we reasoned that a CgA-Aequorin chimera would be trafficked to the chromaffin granules by using the N-terminal targeting information of CgA, and could then monitor free vesicular [Ca^{2+}] under basal or secretion-stimulated conditions. Such a CgA-Aequorin chimera should be useful to probe questions about chromaffin cell Ca^{2+} that have remained elusive for decades, such as: (i) What is the free [Ca^{2+}] in the core of chromaffin granules? (ii) Are chromaffin granule Ca^{2+} stores predominantly free or bound? (iii) How do chromaffin granule Ca^{2+} stores respond to secretory stimuli? (iv) What transporters underlie the accumulation of granular Ca^{2+}? Our studies suggest that chromaffin granules actively accumulate Ca^{2+} against a substantial concentration gradient (vesicle/cytosol), that >99% of Ca^{2+} inside the vesicle remains in bound form, that vesicular [Ca^{2+}] changes promptly in response to secretory stimulation, and that several discrete ion transporters in the granule membrane mediate these processes.

MATERIALS AND METHODS

Plasmids

Cytoplasmic Aequorin (Cyto-Aeq)—The unmodified aequorin coding sequence (open reading frame, Cyto-Aeq), subcloned in the eukaryotic expression vector pcDNA3 (Invitrogen), was a gift from Jenny M. Stables, Glaxo Wellcome, Ware, Herts, United Kingdom.

Human Chromogranin A-Aequorin In-frame Chimera (hCgA-Aeq)—The entire human CgA (hCgA) coding DNA (open reading frame), excluding the stop codon (1371 bp), was first amplified by PCR from the pGEM-hCgA plasmid (from Lee Helman, NCI, National Institutes of Health, Ref. 28) using these forward (5′-CTTCGAATTCTGACCGCCATGCGCTCCGCCGCTGTCCTG-3′, containing the underlined EcoRI site) and backward (5′-CCCGCGGTACCGTGCCCCGCCGTAGTGCCTGCAG-3′, containing the underlined KpnI site) primers. The aequorin-coding region (588 bp) was also amplified by PCR from the Cyto-Aeq plasmid using these forward (5′- CGGGGTACCTATGACCAGCGAACAATACTCAGTC-3′, containing the underlined KpnI site) and backward (5′- ATAAGAATGCGGCCGC GAGTTTCTTAGGGGACAGCTCCACCGTA-3′, containing the underlined NotI site) primers. Following digestion with EcoRI and KpnI, the hCgA PCR product was subcloned between the EcoRI and KpnI sites of the eukaryotic expression vector pEGFP-N1 (containing the CMV immediate-early gene promoter; Clontech, Palo Alto, CA). The KpnI/NotI-digested aequorin PCR product was subsequently ligated between the KpnI and NotI sites of the pEGFP-N1/hCgA plasmid, thereby replacing EGFP, resulting in the hCgA-Aeq plasmid wherein the human CMV promoter drives expression of the fused/in-frame hCgA-Aequorin chimera, with hCgA at the N terminus and aequorin at the C terminus. The correct in-frame fusion of aequorin at the downstream end of hCgA (hCgA-Aeq) was confirmed by sequencing the plasmid construct. Plasmids were grown in *Escherichia coli*, and supercoiled plasmid DNA molecules were purified using Qiagen columns (Qiagen Inc., Chatsworth, CA).

Cell Culture and Transfection

Early passage (passage 8–15) rat pheochromocytoma PC12 cells used in the present study were grown in DME/high glucose medium supplemented with 5% heat-inactivated fetal bovine serum, 10% heat-inactivated horse serum (Gemini Bio-Products, Woodland, CA), 100 unit/ml penicillin G and 100 μg/ml streptomycin (Invitrogen) at 37 °C, 6% CO_2. PC12 cells were transfected with Cyto-Aeq or hCgA-Aeq plasmids by a polycationic lipid method (Superfect; Qiagen, Inc.) as described previously (29).

Subcellular Localization of the Vesicular hCgA-Aeq Chimera: Sucrose Gradient Fractionation and Immunoblotting

PC12 cells grown in 10-cm plates were transfected with hCgA-Aeq. 16 h after transfection, cells were incubated with 1 μCi of [^{3}H]-norepinephrine (PerkinElmer Life Sciences, Inc.) and 5 μM coelenterazine (Molecular Probes, Eugene, OR) for 3 h at 37 °C. Cells were then subjected to three washes with DME/high glucose medium and two washes with PBS, each for 5 min at 37 °C. Cells from three plates were pooled in 3 ml of ice-cold 10 mM HEPES, pH 7.4, 1 mM dithiothreitol, 0.3 M sucrose, and briefly (10–15 s) homogenized by a Tissuemizer (Tekmar, Cincinnati, OH) set at output 50%. The suspension was then layered over a 40 ml continuous sucrose density gradient (0.3- 2.0 M) and centrifuged at 30,000 rpm, 4 °C for 2.5 h (30). 24 samples from different fractions of the sucrose gradient were collected and each fraction was subjected to: (i) [^{3}H]norepinephrine assay (by liquid scintillation counting), (ii) determination of sucrose concentration (by refractometry), and (iii) measurement of aequorin luminescence (to 300 μl of a gradient fraction, 100 μl of 10 mM HEPES, pH 7.4, 400 mM KCl, 40 mM $CaCl_2$, 0.4% Triton X-100 was added by injection, and luminescence was recorded) by a luminometer (Model LB 953, EG&G Berthold.

10 μl of sucrose density gradient fractions were electrophoresed on a 9% SDS-polyacrylamide gel, and the proteins were blotted onto a nitrocellulose membrane. The membrane was incubated overnight at 4 °C with a rat anti-jellyfish aequorin primary antibody (a gift from Larry Ruben, Dallas, TX; 1:500) and for 1 h at room temperature with goat anti-rat IgG conjugated to horseradish peroxidase (1:5000), followed by chemiluminescent detection using an ECL system (Pierce).

Subcellular Localization: Immunolocalization of the Vesicular hCgA-Aeq Chimera

Neurite-differentiated (NGF; 100 ng/ml for 2 days) (31) and control PC12 cells grown on 4 well slides (LabTek, Chamber slides) were transfected with hCgA-Aeq. Neurite-differentiated transfected cells were maintained in NGF (100 ng/ml). The medium was removed 16 h after transfection, washed twice with PBS, and fixed with 2% paraformaldehyde for 1 h at room temperature. PBS-washed cells were permeabilized with 0.1% Triton X-100 in PBS for 5 min and incubated with blocking buffer (0.1% bovine serum albumin, 8 mM glycine in PBS) for 15 min at room temperature. This was followed by incubation with rat anti-jellyfish aequorin primary antibody (1:100) and/or mouse anti-dopamine β-hydroxylase (DBH; 1:150) (BD Pharmingen, San Diego, CA) overnight at 4 °C. Cells were washed twice with PBS (5 min each) and incubated for 1 h at room temperature either with Alexa Fluor® 594 (red) conjugated to goat anti-rat IgG (Molecular Probes, 1:150) to detect hCgA-Aeq, and/or Alexa Fluor® 488 (green) conjugated goat anti-mouse IgG (Molecular Probes, 1:150) to detect DBH. The slides were washed thrice with PBS (10 min each), mounted with ProLong® antifade reagent (Molecular Probes), kept at room temperature for 2 h and stored at 4 °C before viewing under a Zeiss LSM 510 laser scanning confocal microscope.

Secretagogue-stimulated Release of Norepinephrine

Norepinephrine secretion was assayed as described previously (5). In brief, PC12 cells labeled with 1 μCi of L-[^{3}H]norepinephrine for 3 h at 37 °C, washed twice with release buffer (150 mM NaCl, 5 mM KCl, 2 mM $CaCl_2$, 10 mM HEPES pH 7), and incubated for 20 min (at 37 or 8 °C) in release buffer with or without a secretagogue (60 μM nicotine, 100 μM ATP, 1 μM ionomycin, 2 mM $BaCl_2$ or 55 mM KCl). In depolarization experiments, the secretion buffer contained 55 mM KCl and 100 mM NaCl. Precooled (8 °C) release buffer with or without secretagogue was used in low temperature experiments. In some experiments, the release buffer was supplemented with 400 mM sucrose. Supernatant was collected 20 min after treatment, and then the cells were exposed to lysis buffer (150 mM NaCl, 5 mM KCl, 2 mM $CaCl_2$, 10 mM HEPES pH 7, 0.1% (v/v) Triton X-100). Release medium and cell lysates were assayed for [^{3}H]norepinephrine by liquid scintillation counting, and results were expressed as % secretion: (amount released/(amount released + amount in cell lysate)) × 100. Net secretion is secretagogue-stimulated release minus basal release.

Measurement of Aequorin Luminescence and Calibration of [Ca^{2+}]

For *in vivo* experiments, Cyto-Aeq or hCgA-Aeq -transfected PC12 cells were incubated with 5 μM coelenterazine for 1 h in growth medium

at 37 °C for aequorin reconstitution (the process of conversion of apoaequorin into the active photoprotein aequorin via formation of a complex with the luminophore coelenterazine). Cells were washed thrice (5 min each) with modified Krebs-Ringer buffer (KRB; 125 mM NaCl, 5 mM KCl, 1 mM Na_3PO_4, 1 mM $MgSO_4$, 2 mM $CaCl_2$, 5.5 mM glucose, 20 mM HEPES, pH 7.4), scraped gently and suspended in the same KRB. In some experiments, transfected PC12 cells were incubated with coelenterazine in calcium-free KRB (125 mM NaCl, 5 mM KCl, 1 mM Na_3PO_4, 1 mM $MgSO_4$, 5.5 mM glucose, 20 mM HEPES, pH 7.4, 1 mM EGTA) at 37 °C, washed, scraped gently, and suspended in the same calcium-free KRB. Cell suspensions in clear plastic polystyrene 12 × 47 mm tubes were treated with NH_4Cl (1 mM), tyramine (1 mM), bafilomycin A1 (10 nM), thapsigargin (10 μM), amiloride (1 mM), ethyl isopropyl amiloride (10 μM), or KB-R7943 (10 μM) for 20 min at room temperature. The luminescence from Cyto-Aeq or hCgA-Aeq-transfected live cell suspension (mock *versus* treatment) was measured in the 37 °C-heated chamber of an ultra-sensitive, low noise luminometer with a 12W Peltier-cooled (8 °C) photomultiplier tube (PMT), a dark count rate of <100 cps (even at 20 °C), spectral sensitivity of 390–620 nm, 20 ns resolution, and quantum efficiency of 24% (AutoLumat LB 953, EG&G Berthold, Bad Wildbad, Germany), with AutoLumat-PC-Control software in a desktop computer running DOS on an Intel Celeron RAM chip.

The cells received secretagogues (60 μM nicotine, 60 mM KCl, 100 μM ATP, or 1 μM ionomycin) in KRB or calcium-free KRB through software-controlled injector ports. For measurement of aequorin luminescence under basal conditions KRB only was injected to the cell suspension.

In experiments to inhibit exocytosis by low temperature, coelenterazine-reconstituted hCgA-Aeq-expressing PC12 cells were precooled to 8 °C before secretagogue exposure. In experiments to inhibit exocytosis by hyperosmolarity, hCgA-Aeq-expressing PC12 cells were exposed to secretagogues in KRB buffer supplemented with 400 mM sucrose. Luminescence before and after injection of a secretagogue was recorded by the PMT and saved in a Kaleidagraph spreadsheet. At the conclusion of the experiment, activated (unoxidized) aequorin still remaining inside the cells was determined by cell lysis in the presence of 10 mM $CaCl_2$ and 0.05% Triton X-100.

For *in vitro* calibration of aequorin luminescence with respect to free $[Ca^{2+}]$, Cyto-Aeq- or hCgA-Aeq-expressing PC12 cells were reconstituted with coelenterazine (5 μM) in calcium-free KRB, washed with calcium-free KRB, and lysed in calcium-free KRB with 0.05% Triton X-100. The cell lysates (100 μl) were mixed with 100 μl of EGTA-buffered Ca^{2+} solutions (using the on-line MaxChelator program www.stanford.edu/~cpatton/maxc.html), to achieve a range of specific, free $[Ca^{2+}]$ in the final solution), followed by recording of the light emission. The rate of light emission (photon counts per second) was recorded just after addition of a Ca^{2+} buffer (*L*). After 1 min, the cell lysate was exposed to a saturating calcium solution (10 mM $CaCl_2$ in 0.05% Triton X-100) and the recording was continued until the light emission returned to baseline. The luminescence signal at each point of the experiment was normalized by $L_{max,}$ the integral of photon counts from that point to the end of the experiment (32).

For *in vitro* calibration of aequorin luminescence with respect to pH, hCgA-Aeq transfected PC12 cell lysate (100 μl) was mixed with 100 μl of 125 mM NaCl, 5 mM KCl, 1 mM $MgSO_4$, 5.5 mM glucose, and one of the following non-calcium-interacting buffers at 25 mM: MES, pH 5.4; MOPS, pH 6.0; HEPES, pH 7.2, Tris, pH 8.2; glycine, pH 9.6, containing either 0.2 mM or 10 mM $CaCl_2$, followed by recording of luminescence.

Independent Measurement of Cytosolic $[Ca^{2+}]$ by Indo-1 Fluorescence

Indo-1/AM loading solution was freshly prepared as follows: A 50-μg aliquot of Indo-1/AM (Molecular Probes) was mixed with 1.5 μl of a 20% (w/v) Pluronic® F127 solution (low toxicity dispersing agent; Molecular Probes) and 14.5 μl of Me_2SO, yielding a 3 mM solution of Indo-1/AM. This was diluted 1:1000 in Dulbecco's modified Eagle's medium supplemented with 10% fetal bovine serum. To load the cells with Indo-1, PC12 cells grown on LabTek 4-chamber slides having 1 German borosilicate cover glass floor (Nunc) were incubated with 500 μl of loading solution per well at 37 °C in a 5% CO_2 atmosphere for 30 min. After rinsing the cells with KRB, the LabTek chamber was mounted on the stage of a Nikon Diaphot microscope that was interfaced to a Solamere Technologies dual emission photometry system. Excitation was provided by a 100 W mercury lamp and an Indo-1 excitation filter set from Chroma, which features an excitation filter centered at λ_{ex} = 365 nm with a band-pass of 5 nm. A 380 nm dichroic long-pass beam splitter was used under the nose cone of the microscope to separate the excitation and emission fluorescence light pathways. The emission path was split and monitored using separate photomultiplier tubes with band pass emission filters centered at λ_{em} = 405/30 nm or λ_{em} = 485/25, for channel 1 or channel 2, respectively. Data were collected at room temperature at an acquisition rate of 4 Hz with equal gain settings on each channel via a MacLab interface and Power MacIntosh computer using Chart 3.5 software.

For typical experimental runs, the cells were placed in 300 μl of buffer per well. Basal recordings of Indo-1 fluorescence were made from the field of view afforded by a 100× oil-immersion objective. The fields were ~50% confluent and the signals corresponded to data obtained simultaneously from several cells (~20 to 40 per field). Chemicals (*e.g.* nicotine, ATP) were typically added as 300 μl of a 2× stock solution. Following determinations of basal and secretagogue-induced changes in Indo-1 fluorescence, the cells were placed in buffer containing no added calcium with 3 mM EGTA. After ~3 min, this was replaced with a buffer containing no added calcium, with 3 mM EGTA and 10 μM ionomycin. Stable R_{min} values (Indo-1 emission signals at 405 and 485 nm) were obtained within 20 min. During the equilibration with 3 mM EGTA and ionomycin, excitation was intermittent to prevent excessive photobleaching. This buffer was then replaced by a buffer containing 10 mM calcium and 10 μM ionomycin to achieve the R_{max} (equilibration with this buffer was typically achieved within 2 min). Following determination of R_{min} and R_{max}, the buffer was replaced by a buffer containing 10 mM $MnCl_2$, which quenches all Indo-1 fluorescence, resulting in a determination of autofluorescence and background illumination for the field; photomultiplier outputs in the presence of $MnCl_2$ were subtracted from the previously obtained data for each run, post-hoc.

The fluorescence emission (F_{405}/F_{485}) Indo-1 ratio was calibrated to $[Ca^{2+}]_{cyto}$ by the equation: $[Ca^{2+}]_i = K_d\beta(R - R_{min})/(R_{max} - R)$, where the K_d of Indo-1 for calcium was assumed to be 250 nM on the basis of several published reports documenting identical or quite similar K_d values in physiological buffers having ionic strength of ~150 mM and pH of ~7.0 (33–35); β, the ratio of fluorescence obtained at 485 nm, in the absence *versus* the presence of calcium, was 5.16 for this system; and R_{min} and R_{max} were 0.617 and 4.65, respectively.

Chemicals

NH_4Cl, ATP, nicotine, and tyramine were purchased from Sigma. Indo-1/AM (acetoxy-methyl ester), 5-(*N*-ethyl-*N*-isopropyl) amiloride (abbreviated as ethyl-isopropyl amiloride) were obtained from Molecular Probes. 2-[2-[4-(4-nitrobenzyloxy)phenyl]ethyl]isothiourea mesylate (abbreviated as KB-R7943) was purchased from Tocris Cookson Inc. (Ellisville, MO). Amiloride, bafilomycin A1, coelenterazine, ionomycin, and thapsigargin were obtained from Calbiochem (San Diego, CA).

Data Presentation and Statistics

Data are reported as the mean value ± one S.E. One representative result from at least three independent experiments is shown. When only two conditions (*e.g.* control and experimental) were compared, the data were evaluated by unpaired Student's *t* tests. Statistical significance was concluded at $p < 0.05$. Statistics were computed with the programs InStat (GraphPad Software; San Diego, CA), or Kaleidagraph (Synergy/Abelbeck Software; Reading, PA).

RESULTS

Construction and Subcellular Localization of the hCgA-Aeq Chimera—The structure of the hCgA-Aeq chimera is shown in Fig. 1*A*. The construct encodes full-length hCgA and aequorin proteins such that the photoprotein aequorin is fused in-frame at the C terminus of hCgA. The human CMV promoter drives expression of the hCgA-Aeq chimeric protein.

To detect the subcellular localization of the chimera, sucrose density gradient centrifugation was performed on homogenates of PC12 cells transfected with hCgA-Aeq and labeled with [^{3}H]norepinephrine. After centrifugation, we measured sucrose concentration, norepinephrine radioactivity, and aequorin luminescence in different fractions of the gradient. [^{3}H]norepinephrine and aequorin luminescence co-localized in the same gradient fractions with peaks at 1.2 M sucrose (Fig. 1*B*), suggesting that the hCgA-Aeq chimera is trafficked into chromaffin granules in PC12 cells. Consistent with this observation, SDS-PAGE followed by anti-aequorin immunoblotting of the gradient fractions also detected a protein of ~80 kDa (approximately the combined molecular weights of CgA, at ~49 kDa,

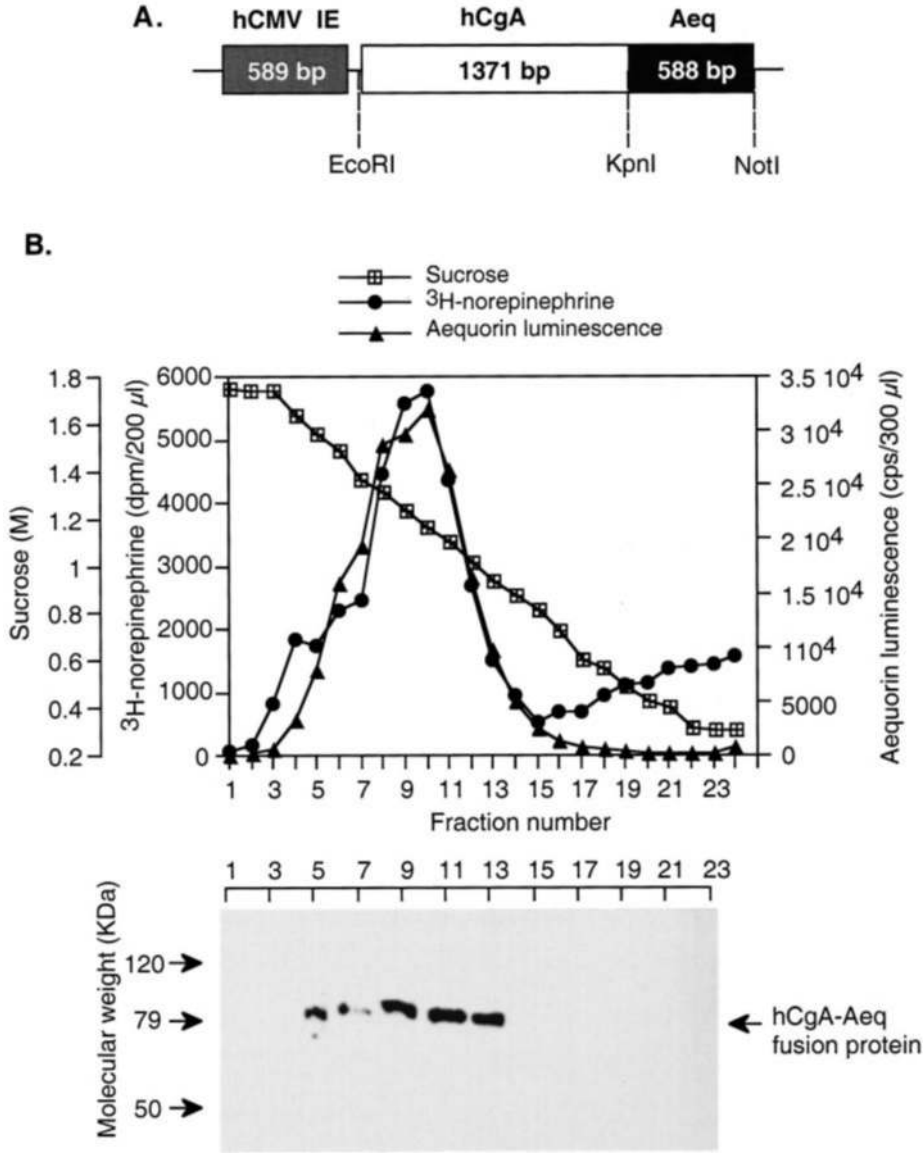

FIG. 1. *A*, schematic map of the hCgA-Aeq. The hCgA cDNA (as an EcoRI-KpnI fragment) is fused with the aequorin (Aeq) cDNA (as a KpnI-NotI fragment) in-frame, and expression of the chimeric gene is driven by the strong human cytomegalovirus immediate-early (*hCMV IE*) promoter. *B*, expression of the hCgA-Aeq fusion protein in PC12 cells and its trafficking to the chromaffin granules. PC12 cells were transfected with hCgA-Aeq, labeled with L-[^{3}H]norepinephrine, homogenized briefly (10–15 s) in isotonic sucrose, and the homogenate was layered over a 40-ml continuous sucrose density gradient (0.3–2.0 M) and centrifuged at 30,000 rpm, 4 °C for 2.5 h. *Top panel*, samples from different fractions of the sucrose gradient were collected and each fraction was subjected to: (i) [^{3}H]norepinephrine assay, (ii) determination of the sucrose concentration (gradient buoyant density position), and (iii) aequorin luminescence measurement. Aequorin luminescence and [^{3}H]norepinephrine counts co-localized in the same subcellular fraction. *Bottom panel*, SDS-PAGE immunoblot of the gradient fractions (using a rat anti-aequorin antibody) detected the hCgA-Aeq fusion protein at M_r ~80.

and aequorin, at ~21–22 kDa) peaking in the same gradient fractions at ~1.2 M sucrose, as shown in Fig. 1*B*.

To confirm appropriate targeting of the hCgA-Aeq fusion protein to chromaffin granules, confocal immunofluorescence microscopy was performed. The hCgA-Aeq fusion protein was visualized with red Alexa Fluor® 594 whereas DBH (chosen as a marker protein of the chromaffin granules) was detected with green Alexa Fluor® 488. The hCgA-Aeq chimera displayed a peripheral pattern typical of secretory granules (Fig. 2*A*, *red*), and co-localized with the distribution pattern of DBH (Fig. 2*B*, *green*); indeed, simultaneous visualization of hCgA-Aeq (red) and DBH (green) yielded nearly complete overlap co-fluorescence (Fig. 2*C*, *yellow*), suggesting co-localization in the same subcellular particle: the chromaffin granule. The immuno-co-localization experiment was also performed with neuron-differentiated PC12 cells; the results demonstrate trafficking of the hCgA-Aeq chimera to DBH-containing granules at the neurite termini (Fig. 2, *D–F*; *arrows*).

Calibration of Aequorin Luminescence with [Ca^{2+}] in Vitro—To convert the aequorin luminescence signal into [Ca^{2+}], we used a series of buffers with different concentrations of free Ca^{2+} and a fixed amount of PC12 cell lysate with expressed Cyto-Aeq or hCgA-Aeq, at constant pH (10 mM HEPES, 0.2 M

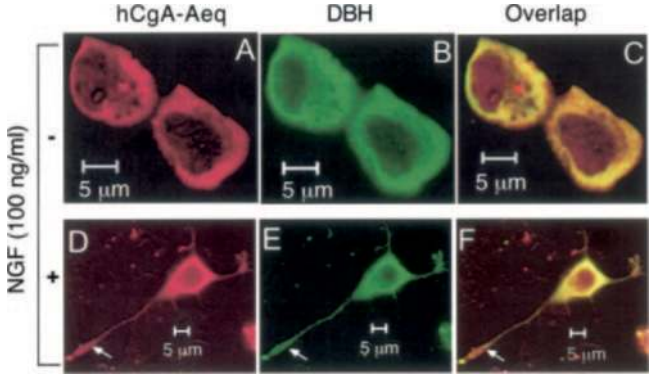

FIG. 2. **Localization of the hCgA-aequorin fusion protein in the chromaffin granules by confocal immunomicroscopy.** Undifferentiated (*A–C*) and neuron-differentiated (*D–F*; NGF, 100 ng/ml, 3 days) PC12 cells transfected with hCgA-Aeq were probed with rat anti-jellyfish aequorin and mouse anti-DBH antibodies, followed by staining with *red* Alexa Fluor® 594 goat anti-rat IgG (to detect the hCgA-Aeq fusion protein; *A* and *D*), or *green* Alexa Fluor® 488 goat anti-mouse IgG (to detect DBH, a marker protein for chromaffin granules; *B* and *E*). Co-localization (in *yellow*) of the hCgA-Aeq fusion protein, and DBH is shown in *C* and *F*. *Arrow*, neurite terminus showing co-localization of hCgA-Aeq and DBH. The original magnification was ×640.

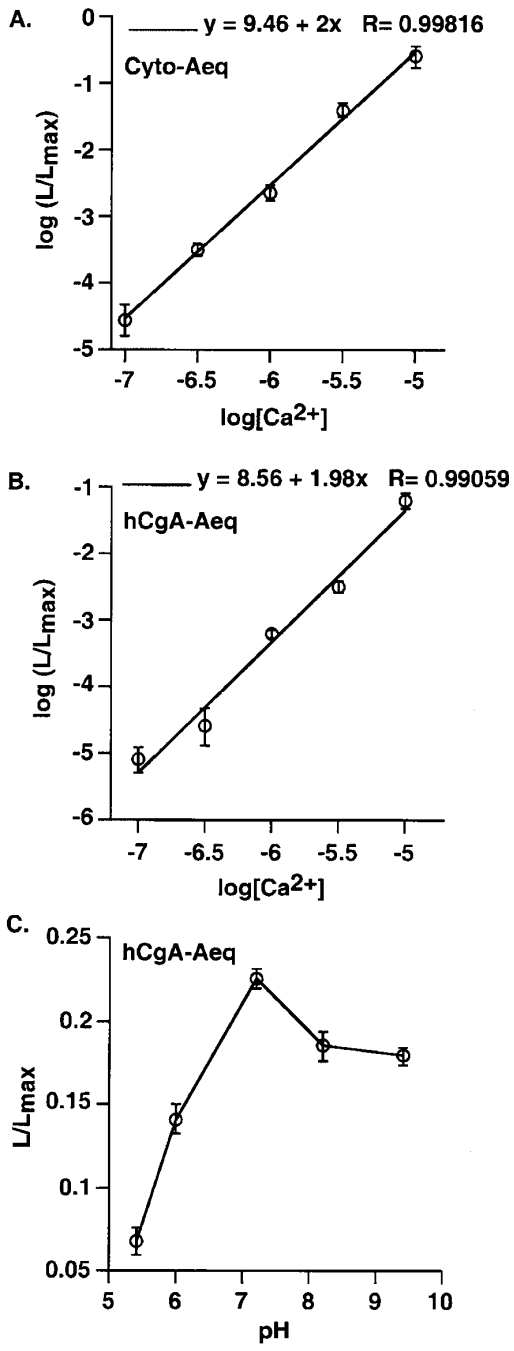

FIG. 3. **Calibration of aequorin luminescence with Ca^{2+} and pH.** *A*, Ca^{2+} response curve of the Cyto-Aeq protein. *B*, Ca^{2+} response curve of the hCgA-Aeq chimeric protein. *C*, pH response curve of the hCgA-Aeq chimeric protein. For determination of calcium response, 100 μl of the Cyto-Aeq- or hCgA-Aeq- transfected PC12 cell lysate was mixed with 100 μl of EGTA-buffered Ca^{2+} solutions followed by recording the light emission continuously. For determination of the pH response, 100 μl of the hCgA-Aeq-expressing PC12 cell lysate was mixed with 100 μl of 125 mM NaCl, 5 mM KCl, 1 mM $MgSO_4$, 5.5 mM glucose, and one of the following pH buffers, at 25 mM: MES, pH 5.4, MOPS, pH 6.0, HEPES, pH 7.2, Tris, pH 8.2, or glycine, pH 9.6. These buffers contained 0.2 mM or 10 mM $CaCl_2$, Luminescence was then recorded. *L* is the rate of photon emission immediately after mixing the cell lysate with the buffer having a particular $[Ca^{2+}]$ or pH, L_{max} is the total remaining light emission at that moment.

KCl, pH 7.0), and plotted the $\log(L/L_{max})$ *versus* $\log[Ca^{2+}]$, where *L* is the rate of light emission just after addition of a particular calcium buffer, and L_{max} is total remaining light emission at that moment. The calcium response curves are shown in Fig. 3, *A* and *B*. For both Cyto-Aeq and hCgA-Aeq, $\log_{10}(L/L_{max})$ linearly predicted $\log_{10}[Ca^{2+}]$ over several orders of magnitude, and down to as low as 10^{-7} M $[Ca^{2+}]$.

Because the chromaffin granule interior is acidified to pH ~5.5 (18, 19), we studied whether aequorin luminescence is influenced by pH, using a series of buffers with different pH values (pH = 5.42–9.40) but a fixed amount of calcium (10 mM), and recombinant hCgA-Aeq. We found that the L/L_{max} values at pH 5.42 were 3.3-fold lower than those at pH 7.2 (Fig. 3*C*). Therefore, to estimate $[Ca^{2+}]$ at pH = 5.5 (approximating the chromaffin granule interior), *in vivo* L/L_{max} values for transfected/expressed hCgA-Aeq were multiplied by the factor 3.3. *In vivo* L/L_{max} values for transfected/expressed Cyto-Aeq were not, of course, so corrected, since physiological cytoplasmic pH is typically ~7.0–7.4.

Based on the $[Ca^{2+}]$ (Fig. 3, *A* and *B*) and pH (Fig. 3*C*) calibrations shown above, algebraic conversion of luminescence values to $[Ca^{2+}]$ was performed by using the following modifications of empirical equations (36): for cytoplasmic free $[Ca^{2+}]$ in molarity, $[Ca^{2+}]_{cyto} = \sqrt{(10^{[x - 9.5]})}$, where $x = \log_{10}(L/L_{max})$; and for the vesicular free calcium in molarity, $[Ca^{2+}]_{ves} = \sqrt{(10^{[y - 8.6]})}$, where $y = \log_{10}(3.3 \times L/L_{max})$.

Comparison of the Cytosolic $[Ca^{2+}]$ Obtained from Cyto-Aeq Luminescence to an Independent Method: Indo-1 Fluorescence—To assure that the equations employed to convert aequorin luminescence to $[Ca^{2+}]$ provide reasonable estimates of free calcium concentration, PC12 cells (same passage) were used to estimate cytoplasmic calcium in two independent ways: by measuring Indo-1 fluorescence (Fig. 4*A*) as well as aequorin luminescence (Fig. 4*C*); in each case, the data were converted to free $[Ca^{2+}]_{cyto}$. Under basal/unstimulated conditions, the free $[Ca^{2+}]_{cyto}$ was found to be 81 ± 10 nM (n = 7 experiments; Fig. 4*B*) as obtained from Indo-1 fluorescence (assuming an Indo-1/Ca^{2+} K_d of 250 nM, Ref. 33), a value which is similar to the $[Ca^{2+}]_{cyto}$ of 130 ± 35 nM (n = 6 experiments, see Table I) as obtained using Cyto-Aeq luminescence.

We also measured the $[Ca^{2+}]_{cyto}$ in the same batch of live PC12 cells after stimulation with a purinergic P_{2x} agonist (100 μM ATP) (5) or a nicotinic cholinergic agonist (60 μM nicotine). After ATP stimulation, the cytosolic $[Ca^{2+}]$ increased to ~1.3 μM (calculated from Indo-1 fluorescence) or ~1.4 μM (calculated from aequorin luminescence) (Fig. 4). Similarly, both techniques could detect an elevation of cytosolic $[Ca^{2+}]$ to ~400 nM after nicotinic stimulation (data not shown). Thus, both basal and peak $[Ca^{2+}]_{cyto}$ values obtained by two different reagents are quite close, suggesting that the aequorin technique bears substantial fidelity to a well established technique (Indo-1 fluorescence) in the cytosol.

Free $[Ca^{2+}]$ in Chromaffin Granules Estimated by hCgA-Aeq Luminescence in Live PC12 Cells—To estimate free intragranular $[Ca^{2+}]$, PC12 cells were transfected with the plasmid hCgA-Aeq, aequorin was reconstituted with coelenterazine 24 h after transfection, and luminescence was recorded continuously in the live cells (Fig. 5, *A* and *C*), with algebraic conversion of luminescence to an estimate of $[Ca^{2+}]_{ves}$ (Fig. 5, *B* and *D*) using the empirical equation derived above: $[Ca^{2+}]_{ves} = \sqrt{(10^{[y - 8.6]})}$, where $y = \log_{10}(3.3 \times L/L_{max})$. We found that free $[Ca^{2+}]_{ves}$ under basal conditions in live PC12 cells in physiological KRB buffer is 1.4 ± 0.31 μM (n = 8 experiments; Table I). In a different set of experiments, when aequorin reconstitution was carried out in the absence of extracellular calcium, injection of 2 mM $CaCl_2$ − supplemented KRB resulted in a transient free $[Ca^{2+}]_{ves}$ peak of 5.8 ± 0.3 μM (n = 6 experiments, Fig. 10), that declined to an intermediate value (lasting for ~10 s) of 2.3 ± 0.2 μM (n = 6 experiments, Fig. 10), followed by a gradual decline to a relatively stable (lasting for several minutes) value of ~1.4 μM (data not shown). Thus, basal free

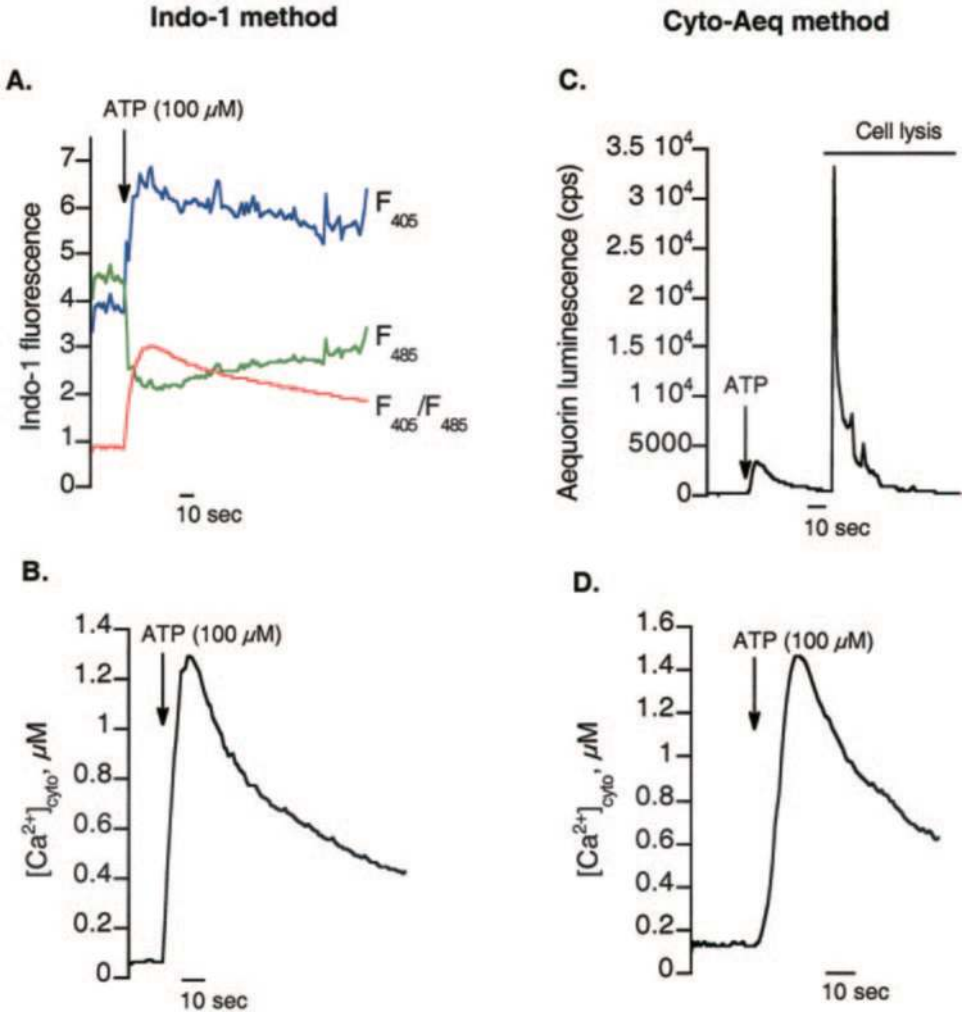

FIG. 4. **Effect of ATP on the cytosolic [Ca^{2+}] as measured by Indo-1 fluorescence and Cyto-Aeq luminescence in live PC12 cells.** *A*, Indo-1 fluorescence at 405 nm (F_{405}, *blue line*) and 485 nm (F_{485}, *green line*), and the ratio (F_{405}/F_{485}, *red line*) before and after stimulation of the PC12 cells with ATP (100 μM). *B*, cytosolic calcium concentration in PC12 cells before and after ATP stimulation as calculated from the Indo-1 fluorescence (shown in *A*). *C*, aequorin luminescence profile of PC12 cells expressing Cyto-Aeq, before and after stimulation with ATP (100 μM) and cell lysis. *D*, effect of ATP on cytosolic calcium concentration as calculated from aequorin luminescence (shown in *C*).

TABLE I

Compartmental [Ca^{2+}] and calecholamine secretion during exocytotic stimulation of PC12 chromaffin cells

Values are shown as mean ± S.E. for replicate observations: $[Ca^{2+}]_{ves}$: Ca^{2+} concentration within chromaffin granules and $[Ca^{2+}]_{cyto}$: Ca^{2+} concentration in the cytosol.

Treatment	Cytosolic and vesicular $[Ca^{2+}]$		Vesicle/cytoplasm $[Ca^{2+}]$ (ratio)	Vesicle-cytoplasm $[Ca^{2+}]$	Ratio: stimulated/basal $[Ca^{2+}]$		Difference: stimulated-basal $[Ca^{2+}]$		Norepinephrine secretion, net % of cell stores
	$[Ca^{2+}]_{cyto}$	$[Ca^{2+}]_{ves}$			$[Ca^{2+}]_{cyto}$	$[Ca^{2+}]_{ves}$	$[Ca^{2+}]_{cyto}$	$[Ca^{2+}]_{ves}$	
	μM			μM			μM		
Basal	0.13 ± 0.035	1.4 ± 0.31	10.8	1.27	—	—	—	—	0
Nicotine (60 μM)	0.42 ± 0.085	1.66 ± 0.12	3.95	1.24	3.2	1.2	0.29	0.26	33.1 ± 0.56
Ionomycin (1 μM)	0.56 ± 0.14	2.62 ± 0.68	4.68	2.06	4.3	1.9	0.43	1.22	25.0 ± 0.36
KCl (60 mM)	0.98 ± 0.17	4.03 ± 0.56	4.11	3.05	7.5	2.9	0.85	2.6	40.1 ± 0.40
ATP (100 μM)	1.4 ± 0.23	9.4 ± 0.98	6.71	8.0	10.7	6.7	1.3	8.0	47.3 ± 2.3

$[Ca^{2+}]_{ves}$ is substantially higher than $[Ca^{2+}]_{cyto}$ (Table I): Vesicle/cytoplasmic ratio = 1.4 μM/0.13 μM = ~10.8-fold higher in the vesicle.

How might chromaffin granule interior pH influence our results? Although chromaffin granule pH is reportedly ~5.5 (18, 19), we did not directly estimate granule pH in these studies. The pH dependence of hCgA-Aeq luminescence (Fig. 3*C*) prompts a pH adjustment in calculation of $[Ca^{2+}]_{ves}$ from raw luminescent counts; at pH = 5.5, the correction factor is 3.3 ($[Ca^{2+}]_{ves} = \sqrt{(10^{[y - 8.6]})}$, where $y = \log_{10}(3.3 \times L/L_{max})$), yielding an estimate of $[Ca^{2+}]_{ves}$ = 1.4 ± 0.31 μM. Based on the degree of pH dependence of hCgA-Aeq (Fig. 3*C*), the corresponding basal $[Ca^{2+}]_{ves}$ estimates at other physiological pH values would be 0.99 μM at pH = 6.0, 0.89 μM at pH = 6.5, and 0.82 μM at pH = 7.0. In each case, the estimated basal free $[Ca^{2+}]_{ves}$ exceeds the basal free $[Ca^{2+}]_{cyto}$ value (at 130 ± 35 nM; Fig. 4 and Table I).

Effect of Chromaffin Cell Secretion on Free [Ca^{2+}] in Cytosol versus Chromaffin Granules—To compare the dynamics of cytosolic and chromaffin granule interior $[Ca^{2+}]$ change upon secretory stimulation, we transfected PC12 cells with Cyto-Aeq or hCgA-Aeq, the aequorins were reconstituted, and the live

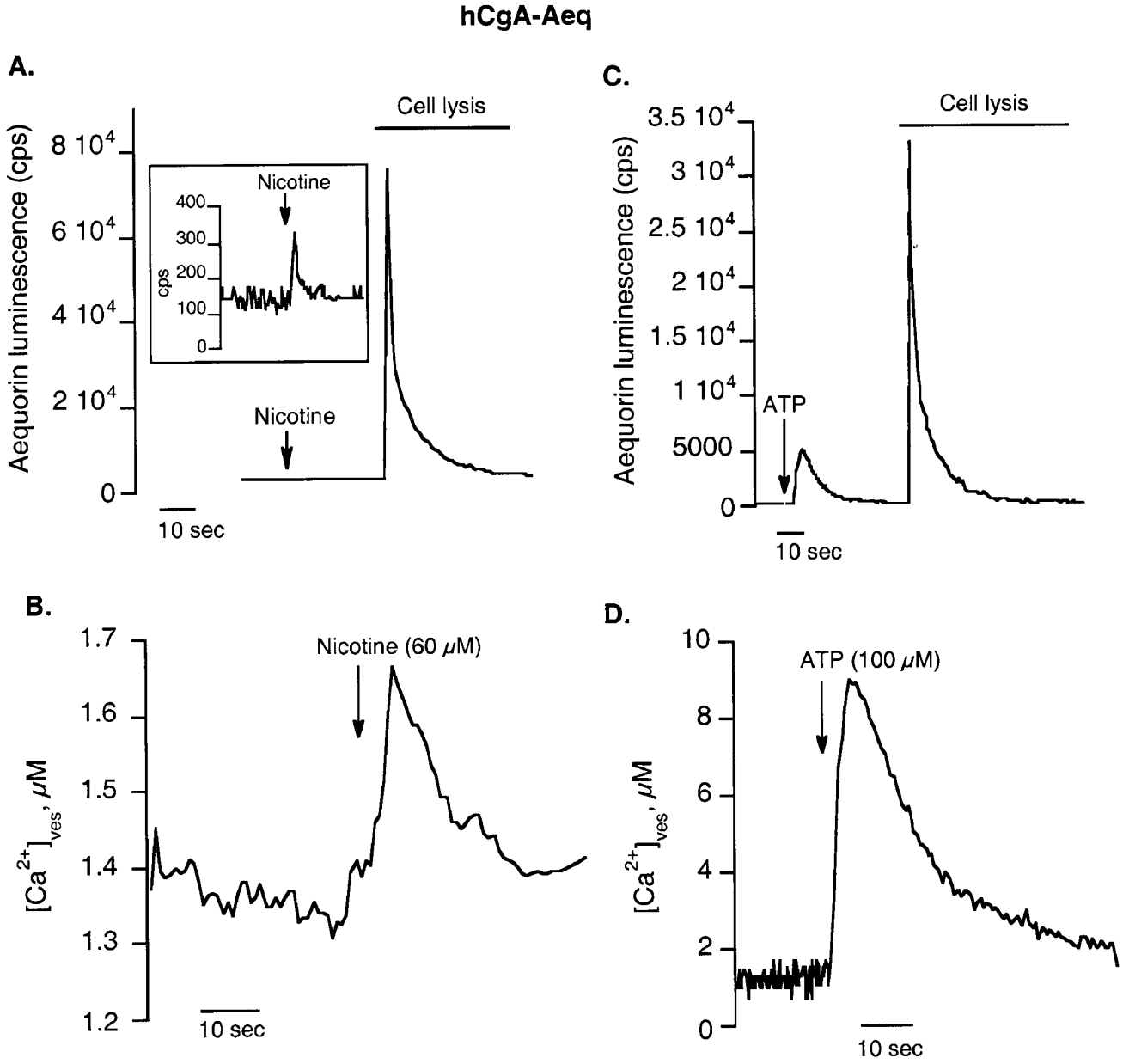

FIG. 5. **Measurement of free calcium concentration inside the chromaffin granules by the hCgA-Aeq chimeric protein.** PC12 cells were transiently transfected with hCgA-Aeq, aequorin was reconstituted by incubation with coelenterazine, cells were suspended in KRB, luminescence was monitored in a luminometer, and the luminescence values were converted to vesicular free calcium concentration as detailed under "Materials and Methods." *A*, aequorin luminescence profile of PC12 cells before and after stimulation with nicotine (60 μM) followed by cell lysis. The *inset* shows an increase in the hCgA-Aeq luminescence upon addition of nicotine with an expanded scale. *B*, calculated vesicular free calcium concentration before and after nicotinic stimulation. *C*, aequorin luminescence profile of PC12 cells before and after stimulation with ATP (100 μM) followed by cell lysis. *D*, calculated vesicular free calcium concentration before and after ATP stimulation.

cells (suspended in KRB) were challenged with customary secretagogues: the nicotinic cholinergic agonist nicotine (60 μM), the purinergic P_{2x} agonist ATP (100 μM) (5), the Ca^{2+} ionophore ionomycin (1 μM), or membrane depolarization (by 60 mM KCl). The secretagogues caused a spectrum of increments in $[Ca^{2+}]_{cyto}$ that drove a logarithmically ascending response of catecholamine secretion ($y = 41.2 + 44.1 \times \log[x]$, $r = 0.96$; where y = % catecholamine secretion and $x = [Ca^{2+}]_{cyto}$ in μM) (Fig. 6), suggesting an approach to saturation of the available exocytotic machinery by pronounced increments in $[Ca^{2+}]_{cyto}$.

Each of these exocytotic stimuli caused increments in both free $[Ca^{2+}]_{cyto}$ and free $[Ca^{2+}]_{ves}$ (Figs. 4, 5, and 7; Table I), the magnitude for both being highest after ATP, rising to 9.4 μM in the granule and 1.4 μM in the cytosol (Fig. 8*A*). The absolute increments (μM, stimulated − basal) in local $[Ca^{2+}]$ during secretion (Table I) were typically greater within vesicles (up to 8.0 μM) than cytosol (up to 1.3 μM), although the stimulated/basal $[Ca^{2+}]$ ratios were somewhat greater in cytosol (3.2 to 10.7) than within vesicles (1.2 to 6.7). Inspection of the relationship between stimulated $[Ca^{2+}]_{ves}$ and $[Ca^{2+}]_{cyto}$ reveals an exponential function ($y = 0.99 \times e^{(1.53x)}$, $r = 0.99$; where $y = [Ca^{2+}]_{ves}$ in μM, and $x = [Ca^{2+}]_{cyto}$ in μM) (Fig. 8*B*), reflecting a persistent $[Ca^{2+}]_{ves}/[Ca^{2+}]_{cyto}$ gradient (at $e^{(1.53x)}$), even during sharp increments of both values (Table I).

These results demonstrate that the calcium pools in both the cytosol and chromaffin granules are dynamic in nature, responding to secretory stimuli; importantly, during secretion there is a prompt and substantial influx of calcium from the cytosol into the granules.

In another set of experiments, after aequorin reconstitution,

PC12 cells transfected with Cyto-Aeq and hCgA-Aeq were subjected to secretory stimulation in the absence of extracellular free $CaCl_2$. No change in the $[Ca^{2+}]_{cyto}$ or $[Ca^{2+}]_{ves}$ was observed after injection of the secretagogues (data not shown); thus, an influx of extracellular calcium seems to be the ultimate source for the increments of both cytoplasmic and vesicular calcium during exocytosis.

Table I summarizes results of studies for both aequorins (Cyto-Aeq to measure $[Ca^{2+}]_{cyto}$, and hCgA-Aeq to measure $[Ca^{2+}]_{ves}$), under both basal and secretagogue-stimulated conditions.

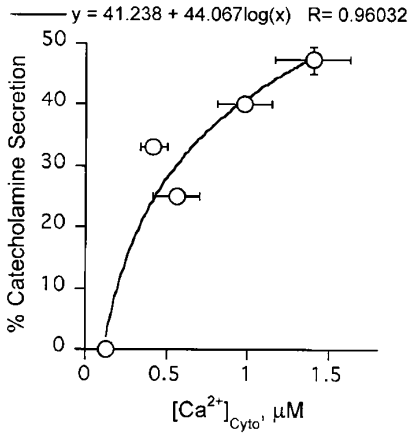

FIG. 6. **Catecholamine secretion as a function of increment in cytosolic $[Ca^{2+}]$ after stimulation.** PC12 cells were stimulated as described under "Materials and Methods," and cytoplasmic $[Ca^{2+}]$ was monitored by Cyto-Aeq luminescence. In a parallel batch of [^{3}H]norepinephrine prelabeled PC12 cells, secretagogue-stimulated transmitter release was monitored by liquid scintillation counting. For the logarithmic fit ($44 \times \log[x]$), $r = 0.96$.

Effect of Extracellular Free Ca^{2+} on Resting Cytosolic versus Chromaffin Vesicular Free $[Ca^{2+}]$—To probe the role of extracellular calcium in determination of cytosolic *versus* vesicular free $[Ca^{2+}]$, PC12 cells transfected with Cyto-Aeq or hCgA-Aeq were aequorin-reconstituted, washed and suspended in calcium-free KRB (that contained 1 mM EGTA), which was then switched to KRB that contained 2 mM $CaCl_2$, during continuous luminescence monitoring (Figs. 9 and 10). Rapid uptake of calcium into cytosol as well as chromaffin vesicle occurred over a time course of ~5 s, transiently raising the $[Ca^{2+}]_{cyto}$ from 150 ± 30 nM to 1.3 ± 0.2 μM ($n = 4$ experiments), and $[Ca^{2+}]_{ves}$ from 1.5 ± 0.3 μM to 5.8 ± 0.3 μM ($n = 8$ experiments) (Figs. 9 and 10). The suggestion is that calcium is accumulated from the extracellular space into cytosol and vesicles even in the basal (unstimulated) state.

Effect of Blockade of Sarcoendoplasmic Reticulum Ca^{2+}-translocating ATPases (SERCAs) on Cytosolic and Vesicular Free $[Ca^{2+}]$—Since basal free $[Ca^{2+}]$ in the chromaffin vesicle was substantially (~10.8-fold) higher than that in the cytosol (Figs. 4 and 5), we explored the role in vesicular calcium accumulation by a Ca^{2+}-translocating ATPase (SERCA pump) on the vesicle membrane, in analogy with SERCA accumulation of calcium in other organelles, such as endoplasmic reticulum (22). We therefore tested the effect of the SERCA inhibitor thapsigargin on cytosolic and vesicular free $[Ca^{2+}]$. PC12 cells transfected with Cyto-Aeq or hCgA-Aeq were coelenterazine-treated for aequorin reconstitution, washed, suspended in calcium-free KRB, and incubated with mock stimulation *versus* 10 μM thapsigargin for 20 min at room temperature, followed by injection of KRB with calcium (final concentration 2 mM). Transient Ca^{2+} uptake into the chromaffin vesicle was significantly reduced by SERCA inhibition: peak free $[Ca^{2+}]_{ves}$ diminished from 5.8 ± 0.3 μM to 3.7 ± 0.1 μM ($n = 4$ experiments), *i.e.* a

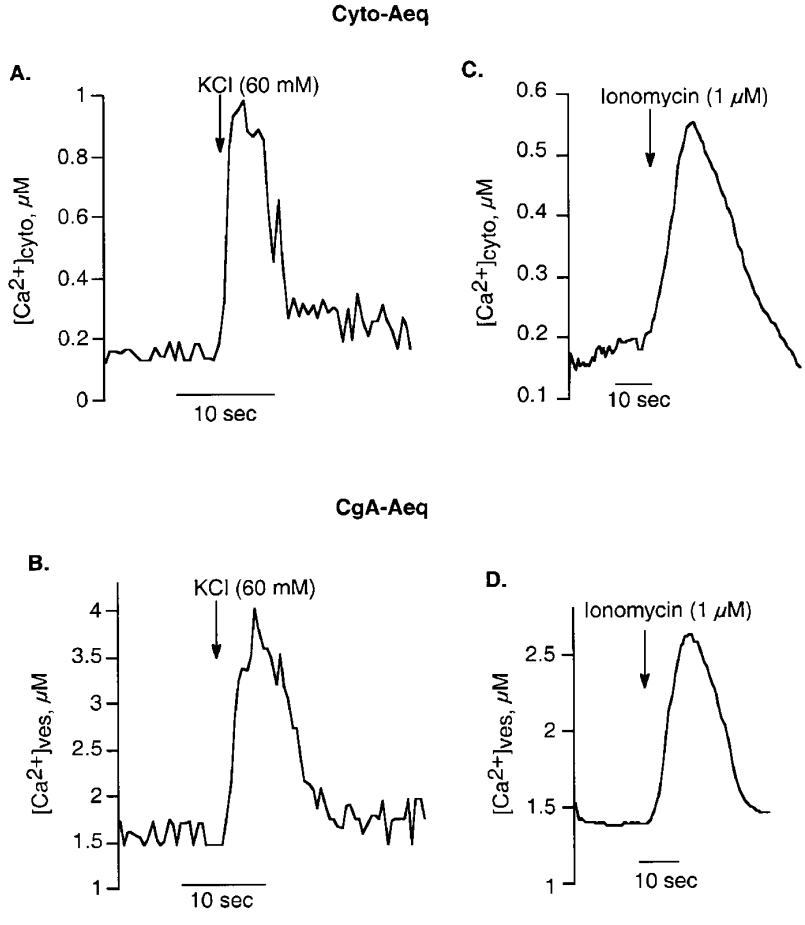

FIG. 7. **Effect of chromaffin cell secretagogues on the cytosolic and vesicular free calcium concentrations.** PC12 cells were transiently transfected with Cyto-Aeq or hCgA-Aeq, aequorin was reconstituted by incubation with coelenterazine, cells were suspended in KRB, followed by injection of KRB alone or KRB plus KCl or KRB plus ionomycin. Luminescence was monitored by a luminometer, and the luminescence values were converted to cytosolic or vesicular free calcium concentration as detailed in the methods. *A*, effect of membrane depolarization by KCl (60 mM) on the $[Ca^{2+}]_{cyto}$ and $[Ca^{2+}]_{ves}$. *B*, effect of the calcium ionophore ionomycin (1 μM) on the $[Ca^{2+}]_{cyto}$ and $[Ca^{2+}]_{ves}$.

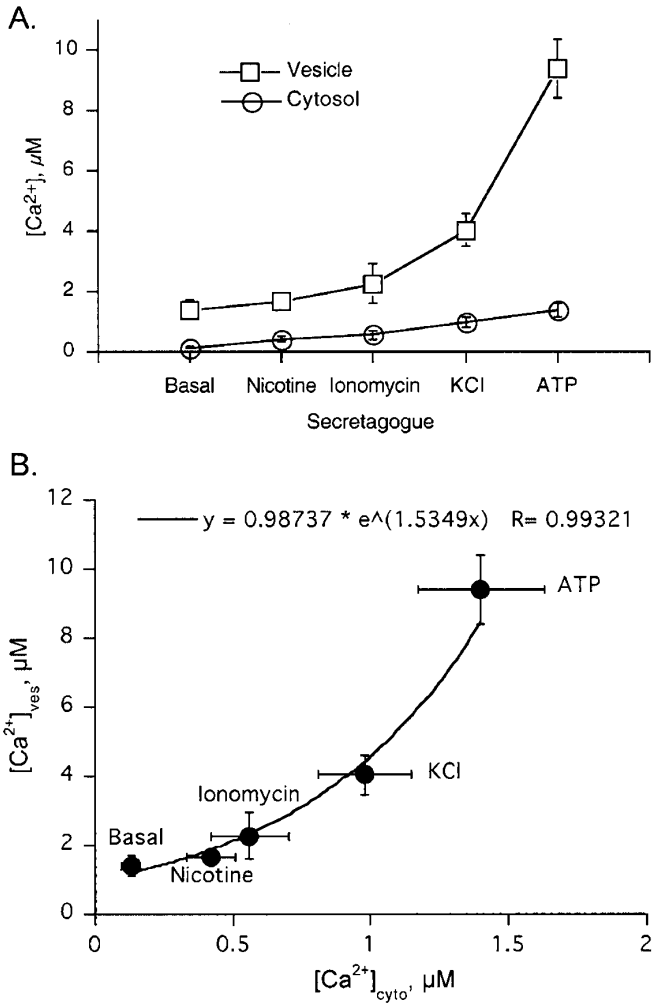

FIG. 8. **Increments in cytosolic and vesicular [Ca^{2+}] during secretory stimulation.** PC12 cells were stimulated as described under "Materials and Methods"; cytoplasmic [Ca^{2+}] was monitored by Cyto-Aeq luminescence, and vesicular [Ca^{2+}] by hCgA-Aeq luminescence. *A*, values for basal and secretagogue-stimulated $[Ca^{2+}]_{cyto}$ and $[Ca^{2+}]_{ves}$ (mean ± S.E.). *B*, $[Ca^{2+}]_{ves}$ as a function of $[Ca^{2+}]_{cyto}$; for the exponential fit ($e^{1.53x}$), $r = 0.99$.

~36.3% decrement upon SERCA inhibition (Fig. 9*A*). On the other hand, the $[Ca^{2+}]_{cyto}$ remained almost unchanged (<10% inhibition) after treatment with thapsigargin (Fig. 9*B*). As a control, injection of KRB *without* calcium had no effect on either cytoplasmic or vesicular calcium concentrations (data not shown). Thus, a SERCA is likely to contribute specifically to calcium accumulation by chromaffin vesicles.

Probing the Role of a Chromaffin Granule Na^+/Ca^{2+} Exchanger (NCX) in Vesicular Calcium Storage—In addition to the plasma membrane, chromaffin granule membranes are also reported to have transmembrane Na^+/Ca^{2+} exchanger (NCX; Na^+/Ca^{2+} antiporter or countertransporter) isoforms (37, 38). To probe the role of NCX, we used the NCX inhibitor KB-R7943, which potently and selectively blocks calcium influx (39). We treated hCgA-Aeq or Cyto-Aeq transfected (aequorin-reconstituted) PC12 cells with KB-R7943 (10 μM) in calcium-free KRB for 20 min prior to injection of calcium (2 mM final concentration). We found that transient Ca^{2+} influx into chromaffin granules was inhibited by ~34.5%, such that peak $[Ca^{2+}]_{ves}$ decreased from 5.8 ± 0.3 μM to 3.8 ± 0.2 ($n = 4$ experiments) μM in the presence of KB-R7943 (Fig. 9*C*). The $[Ca^{2+}]_{cyto}$ peak increment also decreased, from 1.3 ± 0.2 μM to 0.8 ± 0.1 μM ($n = 4$ experiments; Fig. 9*D*). Thus, NCXs seem to mediate calcium influx from the extracellular space in the basal state, ultimately contributing to calcium pools in both the vesicles and the cytoplasm.

Effect of Alkalinization of the Vesicle Core on Cytosolic and Vesicular Free [Ca^{2+}]—Because the chromaffin vesicle is an acidic (pH ~5.5; (18, 19)) compartment, and the low vesicular pH seems to be crucial for vesicular accumulation of cations such as catecholamines (2), we questioned whether there was also a role of pH in control of vesicle [Ca^{2+}]. We probed the role of pH by vesicular alkalinization (with the weak bases NH_4Cl or tyramine), as well as inhibition of the H^+-translocating ATPase by the inhibitor bafilomycin A1 (40).

We incubated aequorin-reconstituted PC12 cells (transfected with Cyto-Aeq or hCgA-Aeq) with NH_4Cl (10 mM) or tyramine (1 mM) for 20 min prior to exposure to 2 mM $CaCl_2$. The peak $[Ca^{2+}]_{ves}$ increment decreased substantially (from 5.8 ± 0.3 μM to 4.0 ± 0.2 μM, $n = 4$ experiments; *i.e.* a ~31.1% decrease) after treatment with either of these alkalinizing agents (Fig. 10*A*). Consistent with this result, 10 nM bafilomycin A1 also decreased peak $[Ca^{2+}]_{ves}$, from 5.8 ± 0.3 μM to 4.1 ± 0.15 μM ($n = 4$ experiments; a ~29.2% decrease, Fig. 10*B*). However, the $[Ca^{2+}]_{cyto}$ was not influenced by either alkalinization procedure (weak base or pump inhibition; data not shown). Thus, the acidic pH in the vesicle core seems specifically to promote vesicular calcium storage.

It should be noted that in these experiments with alkalinizing agents, we used the same algebraic equation employed for estimation of $[Ca^{2+}]_{ves}$ at pH 5.5 (viz. $[Ca^{2+}]_{ves} = \sqrt{(10^{[y\ -\ 8.6]})}$, where $y = \log_{10}(3.3 \times L/L_{max})$ because of the lack of our knowledge on the exact pH upon vesicular alkalinization. However, our pH response curve (Fig. 3*C*) suggests that the calculated $[Ca^{2+}]_{ves}$ values after vesicular alkalinization are overestimated because the multiplication factor at pH >5.5 should then be <3.3. Thus, the limitation of estimating the exact pH upon vesicular alkalinization does not qualitatively affect our finding of lowering of $[Ca^{2+}]_{ves}$ under such conditions.

Role of a Na^+/H^+ Exchanger (NHE) in Granular Ca^{2+} Uptake—Because vesicular pH is important in calcium accumulation (Fig. 10, *A* and *B*), and because H^+ may enter or leave chromaffin granules via a Na^+/H^+ antiporter (41, 42), we evaluated the possibility that such NHEs might influence calcium accumulation by vesicles. We probed involvement of NHEs using specific inhibitors (41, 42), either the weak inhibitor amiloride (1 mM) or the more potent inhibitor ethyl isopropyl amiloride (10 μM). After aequorin reconstitution in calcium-free KRB, hCgA-Aeq- or Cyto-Aeq-transfected PC12 cells were incubated with amiloride for 20 min, followed by injection of 2 mM calcium-containing KRB. In the presence of amiloride, granular Ca^{2+} uptake was inhibited such that the $[Ca^{2+}]_{ves}$ peak decreased by ~19.0%, from 5.8 ± 0.3 μM to 4.7 ± 0.1 μM ($n = 4$ experiments; Fig. 10*C*). The more potent amiloride derivative ethyl-isopropyl amiloride caused more pronounced inhibition of vesicular Ca^{2+} uptake, decreasing peak $[Ca^{2+}]_{ves}$ by ~34.5% to 3.8 ± 0.3 μM ($n = 4$ experiments; Fig. 10*C*). However, cytosolic [Ca^{2+}] remained unchanged after treatment with either amiloride or ethyl-isopropyl amiloride (data not shown). These results suggest that a vesicular Na^+/H^+ antiporter assists in accumulation of [Ca^{2+}] into the vesicle core, a conclusion in accord with studies in chromaffin granule "ghosts" (42).

Are Changes in Vesicle Calcium Concentration during Secretion the Result of Transient Exocytotic Exposure of the Chromaffin Granule Interior to the Extracellular Space?—To investigate this possibility, we stimulated PC12 cells with several typical secretagogues (60 μM nicotine, 100 μM ATP, 60 mM KCl, 1 μM ionomycin, or 2 mM $BaCl_2$) while blocking the very final stage of exocytosis (fusion of docked chromaffin granules to the

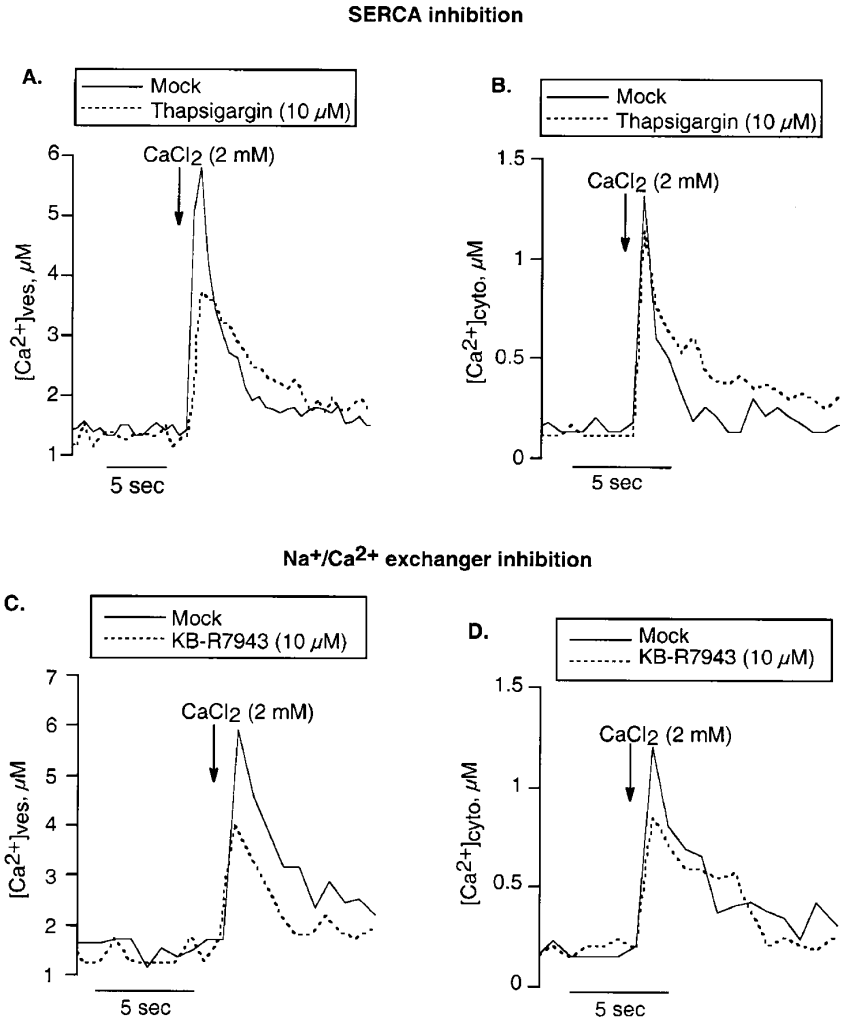

FIG. 9. **Effect of inhibition of Ca^{2+} transporters on the cytosolic and vesicular calcium uptake.** PC12 cells were transfected with Cyto-Aeq or hCgA-Aeq, and aequorin was reconstituted by incubation with coelenterazine in the absence of extracellular Ca^{2+} (with 1 mM EGTA), cells were suspended in calcium-free KRB and incubated with mock solution *versus* a transport inhibitor (the SERCA inhibitor thapsigargin [10 μM], or the NCX inhibitor KB-R7943 [10 μM]) for 20 min, followed by injection of calcium-free KRB or regular KRB containing 2 mM Ca^{2+}. Luminescence was monitored, and photon counts were converted to cytosolic or vesicular free $[Ca^{2+}]$ as detailed under "Materials and Methods." Decrements in vesicular Ca^{2+} uptake were noted after the SERCA inhibitor thapsigargin (*A*), or the NCX inhibitor KB-R7943 (*C*). Inhibition of cytosolic Ca^{2+} uptake was also noted after SERCA inhibition by thapsigargin (*B*), or NCX inhibition by KB-R7943 (*D*).

plasma membrane), at the same time leaving the initial stages in the secretory signaling cascade untouched. We utilized two methods to block the final stage of exocytosis: hyperosmolarity or low temperature (43).

To inhibit exocytosis by hyperosmolarity, PC12 secretion was triggered in Ca^{2+}-containing release buffer supplemented with 400 mM sucrose (43). Such extracellular hyperosmolarity led to substantial decreases in stimulus-triggered net [^{3}H]norepinephrine secretion: by 60% for nicotine, 53% for ATP, 70% for KCl, 47% for ionomycin, or 58% for $BaCl_2$ (Fig. 11*A*). The same batch of PC12 cells was transfected with hCgA-Aeq and after aequorin reconstitution the cells were suspended in KRB *versus* the hyperosmolar buffer (KRB with calcium, plus 400 mM sucrose), followed by determination of the *in vivo* hCgA-Aeq luminescence profile before and after exocytotic secretory stimulation (injection of 100 μM ATP). During exocytosis, the increment in CgA-Aeq luminescence was not affected by hyperosmolarity of the extracellular buffer (Fig. 11*C*), suggesting that secretion-induced changes in granular free $[Ca^{2+}]$ were not simply due to exocytotic exposure of the chromaffin granule interior to the extracellular space, and that the increment in $[Ca^{2+}]_{ves}$ was likely seen in all chromaffin granules, and not just those docked at the plasma membrane awaiting exocytosis.

To inhibit the final stages of exocytosis by hypothermia, we lowered the temperature of the experiment to 8 °C. Previous studies reported blockade of exocytosis at 12 °C (43). However, we found more effective blockade of exocytosis at 8 °C as compared with 12 °C. Secretion from PC12 cells was substantially reduced at 8 °C as compared with that at 37 °C (by 53% for nicotine, 72% for ATP, 67% for KCl, 64% for ionomycin, or 68% for $BaCl_2$; Fig. 11*B*). After aequorin reconstitution, hCgA-Aeq transfected PC12 cells were suspended in KRB with calcium and cooled to 8 °C, followed by stimulation with 100 μM ATP. No diminution of hCgA-Aeq peak luminescence during secretory stimulation was observed during hypothermic blockade of terminal exocytosis (Fig. 11*D*), once again suggesting that the increment in vesicular calcium concentration during secretion was not simply the result of exocytotic exposure of hCgA-Aeq to the extracellular space.

DISCUSSION

Trafficking the hCgA-Aeq Chimera into Chromaffin Granules—The chromaffin granule Ca^{2+} pool has been suggested to play important roles in several cellular events (44, 45), but no reagent to monitor local $[Ca^{2+}]$ in real time in this acidic compartment *in vivo* has heretofore been developed. However, in the recent years, the jellyfish (*Aequorea victoria*) luminescent photoprotein aequorin has been used to measure free $[Ca^{2+}]$ in particular subcellular locations in living cells (21, 22, 46).

Since CgA is the major soluble protein in the interior of chromaffin granules, we reasoned that an expressed hCgA-Aeq chimera would be trafficked into chromaffin granules using CgA targeting signal(s): the well-characterized N-terminal hydrophobic signal peptide, plus additional sequences within the N-terminal domain of the mature protein, which steer it into the regulated secretory pathway (26, 27). Indeed, when PC12 cells were transfected with our expression plasmid hCgA-Aeq,

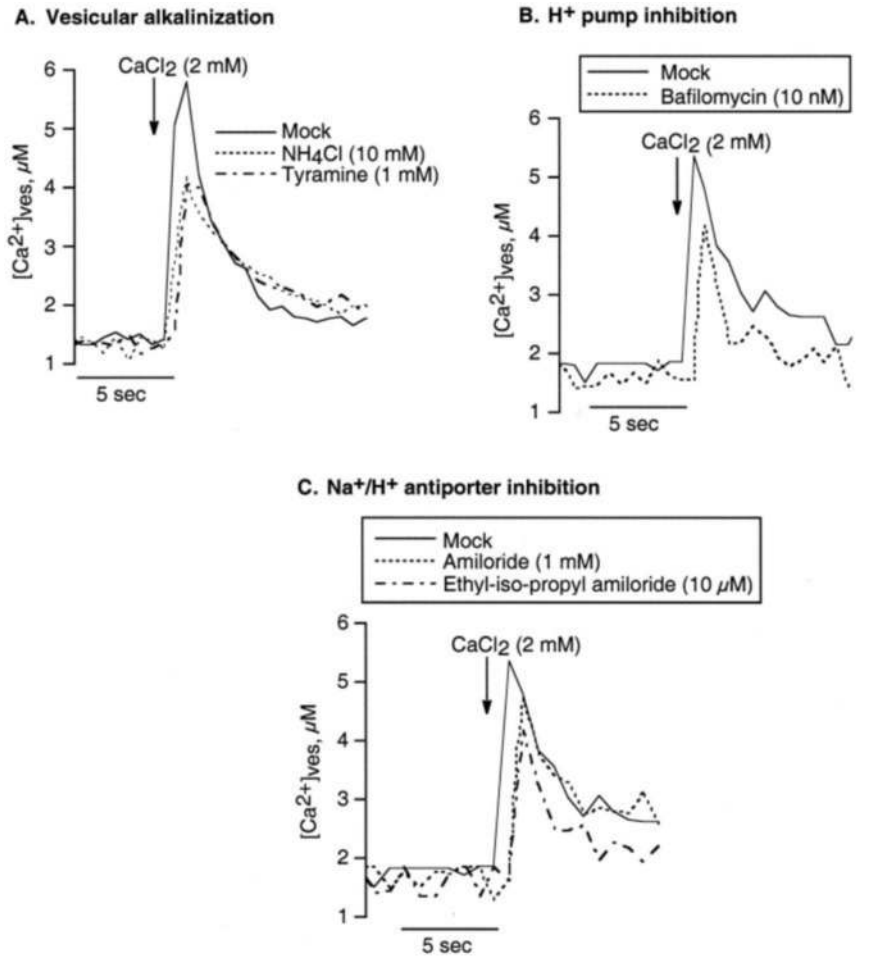

FIG. 10. **Role of protons (H^+) in vesicular Ca^{2+} influx.** Effect of vesicle core alkalinization, inhibition of the H^+-translocating ATPase, or the Na^+/H^+ exchanger on vesicular Ca^{2+} influx. PC12 cells transfected with hCgA-Aeq were subjected to aequorin reconstitution by incubation with coelenterazine in the presence of 1 mM EGTA. The cells were then suspended in calcium-free KRB and incubated with the following: *A*, mock stimulation *versus* the weak bases NH_4Cl (10 mM) or tyramine (1 mM); *B*, mock stimulation *versus* the H^+-pump inhibitor bafilomycin A1 (10 nM); *C*, mock stimulation *versus* the Na^+/H^+ exchanger inhibitors amiloride (1 mM) or ethyl-isopropyl amiloride (10 μm) for 20 min, followed by injection of calcium-free KRB or regular KRB that contained 2 mM Ca^{2+}. Luminescence was monitored, and the photon values were converted to cytosolic or vesicular free $[Ca^{2+}]$ as detailed under "Materials and Methods."

the chimeric protein was correctly trafficked into chromaffin granules, as evidenced by sucrose-density gradient co-sedimentation with catecholamines (Fig. 1), as well as by confocal immunofluorescence microscopic co-localization with the chromaffin granule reference protein dopamine β-hydroxylase (Fig. 2).

Choice of Chimera and Validation of Aequorin Method—Since CgA binds with calcium at high capacity (2) it is most likely that the hCgA-Aeq chimeric protein would bind to calcium. In that case, the hCgA-Aeq may act as a low affinity aequorin probe. Indeed, the L/L_{max} values and hence log (L/L_{max}) values for hCgA-Aeq over a broad range of $[Ca^{2+}]$ are substantially lower than those for the wild-type Cyto-Aeq (Fig. 3, *A* and *B*). Thus, the hCgA-Aeq probe acting like a low affinity aequorin may be advantageous for monitoring $[Ca^{2+}]$ in the chromaffin granules.

Aequorin luminescence *in vitro* was a linear estimator of free $[Ca^{2+}]$ over several orders of magnitude (Fig. 3), and in the cytosol *in vivo* free $[Ca^{2+}]$ ($[Ca^{2+}]_{cyto}$) estimates by aequorin luminescence paralleled those obtained by the fluorescent dye Indo-1 (Fig. 4); thus, the aequorin method was validated by an independent criterion.

Estimation of Free $[Ca^{2+}]$ in Chromaffin Granules within Living PC12 Cells—Our *in vitro* studies indicate that the Cyto-Aeq and the hCgA-Aeq chimeric protein can quantify $[Ca^{2+}]$ linearly down to at least of 0.1 μM (100 nM; Fig. 3); since this sensitivity approximates the concentration of $[Ca^{2+}]$ in the cytosol, we therefore used these aequorins to measure free $[Ca^{2+}]$ in living PC12 cells. We further employed the hCgA-Aeq chimera to estimate local free $[Ca^{2+}]$ concentration in chromaffin granules ($[Ca^{2+}]_{ves}$). Since pH is characteristically quite acidic (pH ~5.5) in the chromaffin granule interior (18, 19), we recalibrated hCgA-Aeq luminescence (Fig. 3*C*) for measurement of $[Ca^{2+}]_{ves}$ at pH 5.5: $[Ca^{2+}]_{ves} = \sqrt{(10^{[y\ -\ 8.6]})}$, where $y = \log_{10}(3.3 \times L/L_{max})$.

Free versus Bound Ca^{2+} in Vesicles—We observed that basal free Ca^{2+} concentration in chromaffin granules in the PC12 cells was 1.4 ± 0.3 μM (Figs. 4, 5, and 7). This figure represents only ~0.004–0.007% of the total granular Ca^{2+} concentration, if the total calcium is estimated to be ~20–40 mM (2). Thus, the great majority (>99.9%) of Ca^{2+} within vesicles would appear to be bound, and thus inaccessible to the local hCgA-Aeq photoprobe for free $[Ca^{2+}]_{ves}$. Haigh *et al.* (41) also investigated Ca^{2+} binding within the chromaffin granule matrix, and concluded that only ~0.03% of granule Ca^{2+} is free (unbound). How is calcium sequestered within the granule core? Our previous *in vitro* studies indicate that CgA itself binds Ca^{2+} electrostatically, at low affinity ($K_d = 1.3 \times 10^{-4}$ M) though high capacity (17 mol Ca^{2+}/mol CgA), and might account for binding of as much as ~94% of Ca^{2+} within the granule core, at the very high prevailing local CgA concentration (2). ATP is also present at substantial concentrations (~150 mM) within chromaffin granules (2); considering that the formation (stability) constants for association of Ca^{2+} with triphosphate are $k_1 = 10^{5.8}$ and $k_2 = 10^{3.7}$ (47), one would predict substantial binding of vesicle Ca^{2+} by ATP *in situ*.

Accumulation of Free Ca^{2+} from Cytosol into Granules—The basal free $[Ca^{2+}]$ in chromaffin granules (1.4 ± 0.31 μM) was ~10.8-fold higher than the basal cytosolic $[Ca^{2+}]$ at 0.13 ± 0.035 μM (Fig. 8*A*; Table I). These observations document a substantial gradient of free $[Ca^{2+}]$ across the granule membrane (granule interior *versus* cytosol), raising the likelihood of

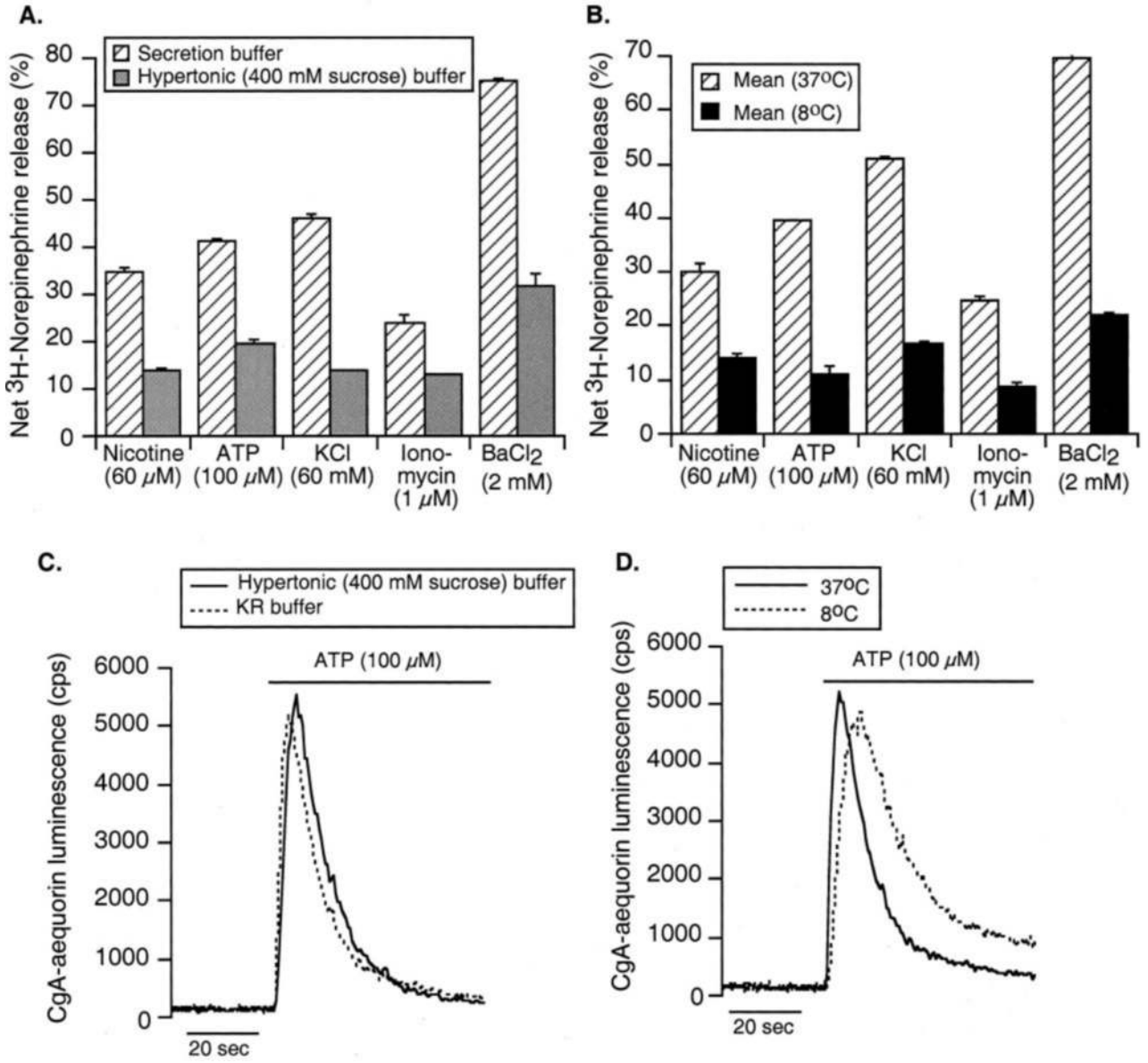

FIG. 11. **Effect of blockade of exocytosis on secretion-induced luminescence of the vesicular hCgA-Aeq chimera in PC12 cells.** *Top panels*, *A*, hCgA-Aeq-expressing PC12 cells were labeled with L-[^{3}H]norepinephrine, and incubated at 37 °C for 20 min with or without a secretagogue, such as nicotine (60 μM), ATP (100 μM), ionomycin (1 μM), KCl (55 mM), or $BaCl_2$ (2 mM), in regular secretion buffer (150 mM NaCl, 5 mM KCl, 2 mM $CaCl_2$, 10 mM HEPES pH 7) or exocytosis-inhibiting hypertonic buffer (400 mM sucrose, 150 mM NaCl, 5 mM KCl, 2 mM $CaCl_2$, 10 mM HEPES pH 7). *B*, hCgA-Aeq-expressing PC12 cells labeled with L-[^{3}H]norepinephrine were incubated at 37 °C or exocytosis-inhibiting low temperature (8 °C) for 20 min with or without a secretagogue in regular secretion buffer. Secretion buffer for experiments involving KCl as secretagogue contained 100 mM NaCl to maintain isotonicity. After 20 min, secretion was terminated by aspirating the secretion buffer, and lysing cells into 150 mM NaCl, 5 mM KCl, 2 mM $CaCl_2$, 10 mM HEPES pH 7, 0.1% (v/v) Triton X-100. Secretion medium and cell lysates were assayed for [^{3}H]norepinephrine secretion by liquid scintillation counting, and results were expressed as % secretion as detailed under "Materials and Methods." *Bottom panels, C*, PC12 cells expressing hCgA-Aeq were aequorin-reconstituted and suspended in KRB (125 mM NaCl, 5 mM KCl, 1 mM Na_3PO_4, 1 mM $MgSO_4$, 2 mM $CaCl_2$, 5.5 mM glucose, 20 mM HEPES, pH 7.4) or KRB supplemented with exocytosis-inhibiting 400 mM sucrose followed by injection of ATP (100 μM). *D*, PC12 cells expressing hCgA-Aeq were aequorin-reconstituted and suspended in KRB and were incubated at 37 °C or exocytosis-inhibiting low temperature (8 °C) prior to and during stimulation with ATP. Aequorin luminescence was monitored continuously before and after addition of ATP.

active calcium accumulation by this organelle.

The Chromaffin Granule Ca^{2+} Pool Is Dynamic during Secretion—We observed that free [Ca^{2+}] in chromaffin granules increased sharply along with an increase of free [Ca^{2+}] in the cytosol, upon stimulation of the cells with exocytotic secretagogues such as nicotine, ATP, KCl, or ionomycin in the presence of extracellular Ca^{2+} (Fig. 8). However, in the absence of extracellular calcium there was no change in granular or cytosolic free [Ca^{2+}] after challenge with these agonists (data not shown), suggesting that an influx of Ca^{2+} from the extracellular medium first into the cytosol and in turn from the cytosol into the granules is required for the secretion-associated granular Ca^{2+} increment. Thus, chromaffin granules seem to remove Ca^{2+} from the cytosol during secretion, rather than releasing Ca^{2+} into the cytosol during this process. A modest general decline in the vesicle/cytosol [Ca^{2+}] ratios during secretion (from 10.8 down to 3.95 to 6.71; Table I) is also in line of this suggestion. Hence, the transient increment of $[Ca^{2+}]_{ves}$ during secretion (Figs. 5 and 7) is likely to be a response to cytosolic Ca^{2+} fluxes during secretion, rather than a contributor to secretion. The exponential relationship between $[Ca^{2+}]_{ves}$ and $[Ca^{2+}]_{cyto}$ ($y = 0.99 \times e^{(1.53x)}$, $r = 0.99$; where $y = [Ca^{2+}]_{ves}$

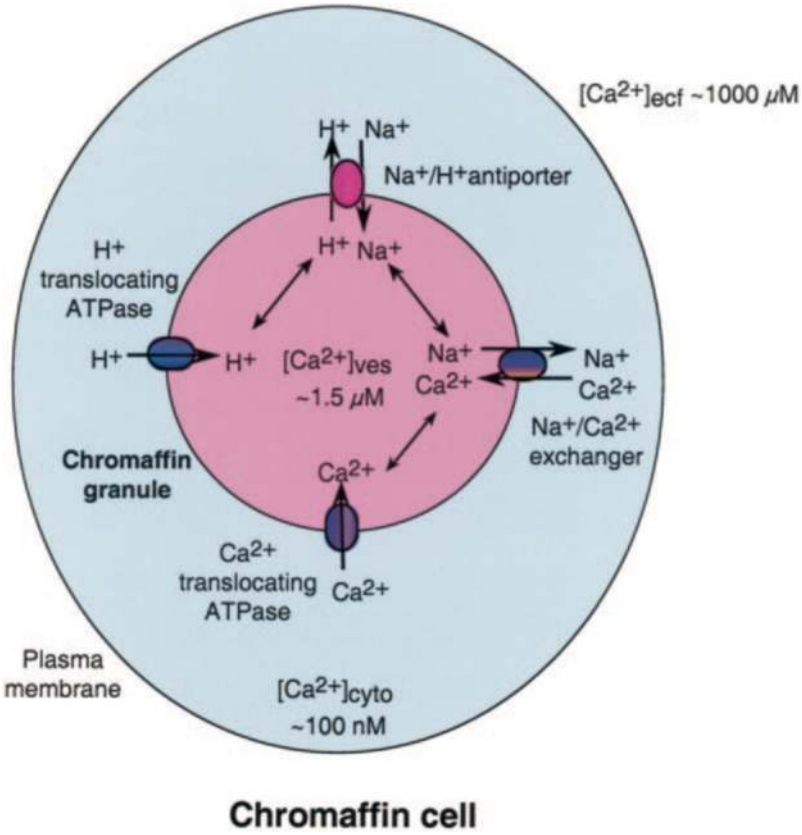

FIG. 12. **Model for Ca^{2+} accumulation within catecholamine storage vesicles (chromaffin granules) of chromaffin cells.** Putative chromaffin granule membrane ion channels underlying calcium transport and storage are illustrated, in accordance with the data generated in this report. $[Ca^{2+}]_{ves}$, free calcium concentration within the catecholamine storage vesicle. $[Ca^{2+}]_{cyto}$, free calcium concentration within the cytosol. $[Ca^{2+}]_{ecf}$, free calcium concentration in the extracellular fluid (space).

in μM, and $x = [Ca^{2+}]_{cyto}$ in μM) (Fig. 8*B*) indicates that the granule is able to maintain a Ca^{2+} concentration gradient over rather extreme ranges.

Thus, the chromaffin granule was able to maintain a substantial $[Ca^{2+}]$ storage gradient over cytosol during stimulated secretion (Table I); indeed, during the most extreme stimulation (by ATP; Table I, Fig. 8*A*) the absolute (μM) increment in vesicular $[Ca^{2+}]$ far exceeded that in cytosolic $[Ca^{2+}]$. Hence, the active accumulation mechanism(s) for calcium into chromaffin granules follows kinetics comparable to those for cytosolic Ca^{2+} transients during secretion (Fig. 8). By contrast, Haigh and Phillips (42) found that Ca^{2+} uptake into isolated chromaffin granule ghosts *in vitro* was relatively slow; the isolated membranes might lack participating components of the intact transport system *in vivo*.

Ca^{2+} Influx into Chromaffin Granules: Dependence on a Ca^{2+}-translocating ATPase (SERCA) and Na^+/Ca^{2+} Exchanger (NCX)—To explore the role of particular Ca^{2+} transporters in Ca^{2+} influx into granules, we blocked SERCAs by thapsigargin (48) (Fig. 9*A*) and NCXs by KB-R7943 (39) (Fig. 9*C*). Both the inhibitors substantially decreased Ca^{2+} uptake into the granules, and in each case the effects were more pronounced for granular than cytoplasmic Ca^{2+} (Fig. 9, *B* and *D*).

The presence of NCXs on chromaffin granule membranes has been suggested by both functional evidence (42, 43, 49) and identification of specific NCX1 transcript isoforms in chromaffin cells (38, 50), and Haigh and Phillips (42) reported indirect evidence for a role of NCXs in Ca^{2+} accumulation by chromaffin granule ghosts. Our results with the "influx" mode inhibitor KB-R7943 (Fig. 9*C*) are consistent with such a role for NCX in vesicular Ca^{2+} uptake.

Diminution of peak Ca^{2+} uptake by granules in the presence of the SERCA inhibitor thapsigargin (Fig. 9*A*) suggests a SERCA on the granule membrane. While SERCAs are widely established as mediators of calcium uptake in the endoplasmic reticulum of chromaffin cells (51), SERCAs on the chromaffin granule membrane are not conclusively established by our pharmacologic data (Fig. 9*A*) and await molecular confirmation.

Role of Granule H^+ Transporters and pH—Since the acidic pH compartment within chromaffin granules is crucial to accumulation of catecholamines (2), we evaluated the effects of H^+ gradient (Fig. 10, *A* and *B*) or H^+ transport (Fig. 10*C*) disruption on vesicular Ca^{2+} storage. Indeed, disruption of the acidic pH of the granule core (Fig. 10, *A* and *B*) impaired the ability of granules to accumulate Ca^{2+}, whether the granule pH gradient was diminished by weak bases (Fig. 10*A*) or H^+ pump inhibition (Fig. 10*B*); lack of effect of these procedures on cytosolic $[Ca^{2+}]$ reinforces their specificity for granule events. The implication is that the chromaffin granule membrane H^+-translocating ATPase plays an active role in Ca^{2+} accumulation by the granule.

Similarly, inhibition of Na^+/H^+ exchange (Fig. 10*C*) impaired the ability of granules to accumulate Ca^{2+}, even without changes in cytosolic $[Ca^{2+}]$. Indirect (pharmacologic) evidence (41) has previously been presented for a functional Na^+/H^+ exchanger (NHE) on the chromaffin granule membrane (though the particular NHE isoform is not established), and the Na^+/H^+ antiporter may assist in coupling Ca^{2+} transport to H^+ translocation into chromaffin granule ghosts (42).

Role of Exocytotic Exposure of the Luminophore—The luminescence increments of vesicular hCgA-Aeq during stimulation of secretion were not blunted during blockade of the final stage of exocytosis, using the tools of hyperosmolarity or low temperature (Fig. 11); hence, the vesicular $[Ca^{2+}]$ increments observed are authentic responses to cytosolic transients early in the secretory process, and do not simply represent increments in luminescence consequent upon late exocytotic exposure to the higher $[Ca^{2+}]$ in the extracellular space.

Comparison to Other Studies of Ca^{2+} Transport in Pancreatic Insulin Secretory Granules or Chromaffin Granules—In a series of studies of Ca^{2+} storage in insulin secretory granules of

pancreatic islet β-cells, using an aequorin targeted to the granule interior by the vesicle associated membrane protein VAMP2 (synaptobrevin), Mitchell *et al.* (52–54) describe somewhat different mechanisms and significance of Ca^{2+} accumulation and release by secretory vesicles.

Mitchell *et al.* (52) estimated that basal free vesicular [Ca^{2+}] was substantially higher in insulin vesicles, at ~40–50 μM, but this value fell greatly in the absence of extracellular Ca^{2+}; these findings are quite different from our observations in chromaffin granules. Furthermore, Mitchell *et al.* (52) found no effects of bafilomycin (H^+ pump inhibitor), FCCP (protonophore), thapsigargin (SERCA inhibitor), monensin (Na^+/H^+ exchange inhibitor), or ionomycin (Ca^{2+} ionophore, Ca^{2+}/H^+ exchanger) on granule [Ca^{2+}]. These observations suggest that granule Ca^{2+} accumulation mechanisms are qualitatively different in insulin (52–54) *versus* chromaffin granules (the present report). Since previous studies of chromaffin granules have already suggested roles for NHEs (41) and NCXs (42, 49) in vesicular Ca^{2+} storage, consistent with our results, it appears that the observed differences in Ca^{2+} storage mechanisms between insulin granules and chromaffin granules are authentic.

Using the technique of RNA silencing, Mitchell *et al.* (54) later documented a role for a novel, SERCA inhibitor-insensitive (52) Ca^{2+}-ATPase: ATP2C1 (rodent ortholog: PMR1). Intriguingly, PMR1 depletion inhibited Ca^{2+} uptake into secretory vesicles while augmenting secretion, perhaps indicating that the role of Ca^{2+} accumulation by granules might play a braking or terminating role in secretion, rather than contributing to secretion, a suggestion in line with our findings.

Mitchell *et al.* (53) also probed the possible role of two vesicular receptors in Ca^{2+} accumulation or release by isolated insulin secretory granules: the ryanodine receptor type I (RyR-I) and a nicotinic acid adenine dinucleotide phosphate (NAADP) receptor. Inhibition of RyR-I by dantrolene elevated vesicular [Ca^{2+}] over 2-fold, while inhibiting insulin secretion, suggesting that vesicular Ca^{2+} might contribute to the secretory process. NAADP decreased vesicular [Ca^{2+}], releasing the ion from vesicular stores. Our studies in intact, living cells were not amenable to such *in vitro* perturbations.

In isolated chromaffin granules, Yoo *et al.* (55) have provided indirect evidence for an inositol 1,4,5-trisphosphate receptor/Ca^{2+} channel in the granule membrane, suggesting that chromaffin granules may be a source of Ca^{2+} to be delivered to the cytosolic exocytotic machinery during secretion. While documenting active Ca^{2+} storage in the chromaffin granule (Table I and Fig. 8), our results favor a role of the chromaffin granule *in response to* exocytosis, rather than in stimulation of exocytosis.

Model for Ca^{2+} Storage in the Chromaffin Granule—To accommodate our experimental findings, we propose the following model of active Ca^{2+} accumulation, against a concentration gradient ($[Ca^{2+}]_{ves}/[Ca^{2+}]_{cyto}$), by the chromaffin granule (Fig. 12). Ca^{2+} is accumulated against a ~10.8-fold concentration gradient, $[Ca^{2+}]_{ves}/[Ca^{2+}]_{cyto}$. The driving force behind the $[Ca^{2+}]_{ves}/[Ca^{2+}]_{cyto}$ gradient is likely to be a Ca^{2+}-translocating ATPase in the granule membrane. Ca^{2+} can also enter the granule via a Na^+/Ca^{2+} exchanger in the membrane. Ca^{2+} transport across the Na^+/Ca^{2+} exchanger should also be influenced by the granule interior concentration of the co-substrate Na^+, which in turn is also affected by the activity of a granule membrane Na^+/H^+ exchanger. Finally, Na^+ transport across the Na^+/H^+ exchanger is determined by the granule interior concentration of the co-substrate H^+, whose concentration also depends on the activity of a granule membrane H^+-translocating ATPase. Of note, although the present study clearly indicated involvement of multiple transporters in the process of calcium influx into the granules, their relative contributions remain to be explored. It is conceivable that one of these carriers play a predominant role over the others; indeed, while passive ion transporters such as the NCX or the NHE catalyze ion movements in response to concentration gradients, it is likely that active, energy-consuming generators of vesicular ion gradients, such as the SERCA and the H^+-ATPase, would determine the initial or set point for calcium fluxes. Within the realm of active transporters, SERCA inhibition achieved the greatest inhibition of calcium flux (by ~36.3%; Fig. 9*A*). This novel model for Ca^{2+} accumulation within the chromaffin granule should prove useful in design of future experiments to confirm or refute the presence of specific transport carriers in the underlying such processes in the granule membrane.

REFERENCES

1. Winkler, H., and Fischer-Colbrie, R. (1992) *Neuroscience* **49,** 497–528
2. Videen, J. S., Mezger, M. S., Chang, Y. M., and O'Connor, D. T. (1992) *J. Biol. Chem.* **267,** 3066–3073
3. Taupenot, L., Harper, K. L., and O'Connor, D. T. (2003) *New Engl. J. Med.* **348,** 1134–1149
4. Douglas, W. W. (1968) *Br. J. Pharmacol.* **34,** 453–474
5. Mahata, S. K., O'Connor, D. T., Mahata, M., Yoo, S. H., Taupenot, L., Wu, H., Gill, B. M., and Parmer, R. J. (1997) *J. Clin. Investig.* **100,** 1623–1633
6. Tang, K., Wu, H., Mahata, S. K., Mahata, M., Gill, B. M., Parmer, R. J., and O'Connor, D. T. (1997) *J. Clin. Investig.* **100,** 1180–1192
7. West, A. E., Chen, W. G., Dalva, M. B., Dolmetsch, R. E., Kornhauser, J. M., Shaywitz, A. J., Takasu, M. A., Tao, X., and Greenberg, M. E. (2001) *Proc. Natl. Acad. Sci. U. S. A.* **98,** 11024–11031
8. Dolmetsch, R. E., Pajvani, U., Fife, K., Spotts, J. M., and Greenberg, M. E. (2001) *Science* **294,** 333–339
9. Hilfiker, S. (2003) *Biochem. Soc. Trans* **31,** 828–832
10. Berridge, M. J. (1998) *Neuron* **21,** 13–26
11. Villalobos, C., Nunez, L., Montero, M., Garcia, A. G., Alonso, M. T., Chamero, P., Alvarez, J., and Garcia-Sancho, J. (2002) *FASEB J.* **16,** 343–353
12. Herrington, J., Park, Y. B., Babcock, D. F., and Hille, B. (1996) *Neuron* **16,** 219–228
13. Filippin, L., Magalhaes, P. J., Di Benedetto, G., Colella, M., and Pozzan, T. (2003) *J. Biol. Chem.* **278,** 39224–39234
14. Park, Y. B., Herrington, J., Babcock, D. F., and Hille, B. (1996) *J. Physiol.* **492,** 329–346
15. Machado, J. D., Segura, F., Brioso, M. A., and Borges, R. (2000) *J. Biol. Chem.* **275,** 20274–20279
16. Herrero, C. J., Ales, E., Pintado, A. J., Lopez, M. G., Garcia-Palomero, E., Mahata, S. K., O'Connor, D. T., Garcia, A. G., and Montiel, C. (2002) *J. Neurosci.* **22,** 377–388
17. Miyawaki, A., Llopis, J., Heim, R., McCaffery, J. M., Adams, J. A., Ikura, M., and Tsien, R. Y. (1997) *Nature* **388,** 882–887
18. Johnson, R. G., and Scarpa, A. (1976) *J. Biol. Chem.* **251,** 2189–2191
19. Casey, R. P., Njus, D., Radda, G. K., and Sehr, P. A. (1977) *Biochemistry* **16,** 972–977
20. Chiesa, A., Rapizzi, E., Tosello, V., Pinton, P., de Virgilio, M., Fogarty, K. E., and Rizzuto, R. (2001) *Biochem. J.* **355,** 1–12
21. Brini, M., Pinton, P., Pozzan, T., and Rizzuto, R. (1999) *Microsc. Res. Tech* **46,** 380–389
22. Montero, M., Brini, M., Marsault, R., Alvarez, J., Sitia, R., Pozzan, T., and Rizzuto, R. (1995) *EMBO J.* **14,** 5467–5475
23. Rizzuto, R., Simpson, A. W., Brini, M., and Pozzan, T. (1992) *Nature* **358,** 325–327
24. Pinton, P., Pozzan, T., and Rizzuto, R. (1998) *EMBO J.* **17,** 5298–5308
25. Brini, M., Murgia, M., Pasti, L., Picard, D., Pozzan, T., and Rizzuto, R. (1993) *EMBO J.* **12,** 4813–4819
26. Parmer, R. J., Xi, X. P., Wu, H. J., Helman, L. J., and Petz, L. N. (1993) *J. Clin. Investig.* **92,** 1042–1054
27. Taupenot, L., Harper, K. L., Mahapatra, N. R., Parmer, R. J., Mahata, S. K., and O'Connor, D. T. (2002) *J. Cell Sci.* **115,** 4827–4841
28. Helman, L. J., Ahn, T. G., Levine, M. A., Allison, A., Cohen, P. S., Cooper, M. J., Cohn, D. V., and Israel, M. A. (1988) *J. Biol. Chem.* **263,** 11559–11563
29. Mahapatra, N. R., Mahata, M., Datta, A., Gerdes, H.-H., Huttner, W. B., O'Connor, D. T., and Mahata, S. K. (2000) *Endocrinology* **141,** 3668–3678
30. Aberer, W., Stitzel, R., Winkler, H., and Huber, E. (1979) *J. Neurochem.* **33,** 797–801
31. Mahata, S. K., Mahata, M., Wu, H., Parmer, R. J., and O'Connor, D. T. (1999) *Neuroscience* **88,** 405–424
32. Brini, M., Marsault, R., Bastianutto, C., Alvarez, J., Pozzan, T., and Rizzuto, R. (1995) *J. Biol. Chem.* **270,** 9896–9903
33. Grynkiewicz, G., Poenie, M., and Tsien, R. Y. (1985) *J. Biol. Chem.* **260,** 3440–3450
34. Lattanzio, F. A., Jr. (1990) *Biochem. Biophys. Res. Commun.* **171,** 102–108
35. Kagaya, Y., Weinberg, E. O., Ito, N., Mochizuki, T., Barry, W. H., and Lorell, B. H. (1995) *J. Clin. Investig.* **95,** 2766–2776
36. Rutter, G. A., Theler, J. M., Murgia, M., Wollheim, C. B., Pozzan, T., and Rizzuto, R. (1993) *J. Biol. Chem.* **268,** 22385–22390
37. Tang, Y. M., Travis, E. R., Wightman, R. M., and Schneider, A. S. (2000) *J. Neurochem.* **74,** 702–710
38. Schneider, A. S., Mah, S. J., Farhadi, M., Grindi, E., and Davis, K. H. (2002) *Ann. N. Y. Acad. Sci.* **971,** 142–144

39. Shigekawa, M., and Iwamoto, T. (2001) *Circ. Res.* **88,** 864–876
40. Machado, J. D., Gomez, J. F., Betancor, G., Camacho, M., Brioso, M. A., and Borges, R. (2002) *Circ. Res.* **91,** 830–836
41. Haigh, J. R., Parris, R., and Phillips, J. H. (1989) *Biochem. J.* **259,** 485–491
42. Haigh, J. R., and Phillips, J. H. (1993) *Neuroreport* **4,** 571–574
43. Jan, C. R., and Schneider, A. S. (1992) *J. Biol. Chem.* **267,** 9695–9700
44. Yoo, S. H. (2000) *Trends Neurosci.* **23,** 424–428
45. Yoo, S. H., and Lewis, M. S. (1996) *J. Biol. Chem.* **271,** 17041–17046
46. Robert, V., Pinton, P., Tosello, V., Rizzuto, R., and Pozzan, T. (2000) *Methods Enzymol.* **327,** 440–456
47. Dawson, R. M. C., Elliott, D. C., Elliott, W. H., and Jones, K. M. (1986) *Data for Biochemical Research*, 3rd Ed., pp. 6–7, Oxford University Press, New York
48. Lytton, J., Westlin, M., and Hanley, M. R. (1991) *J. Biol. Chem.* **266,** 17067–17071
49. Phillips, J. H. (1981) *Biochem. J.* **200,** 99–107
50. Pan, C. Y., Chu, Y. S., and Kao, L. S. (1998) *Biochem. J.* **336,** 305–310
51. Rigual, R., Montero, M., Rico, A. J., Prieto-Lloret, J., Alonso, M. T., and Alvarez, J. (2002) *Eur. J. Neurosci.* **16,** 1690–1696
52. Mitchell, K. J., Pinton, P., Varadi, A., Tacchetti, C., Ainscow, E. K., Pozzan, T., Rizzuto, R., and Rutter, G. A. (2001) *J. Cell Biol.* **155,** 41–51
53. Mitchell, K. J., Lai, F. A., and Rutter, G. A. (2003) *J. Biol. Chem.* **278,** 11057–11064
54. Mitchell, K. J., Tsuboi, T., and Rutter, G. A. (2004) *Diabetes* **53,** 393–400
55. Yoo, S. H., So, S. H., Huh, Y. H., and Park, H. Y. (2002) *Ann. N. Y. Acad. Sci.* **971,** 300–310